

Supplementary Information

A design principle underlying the paradoxical roles of E3 ubiquitin ligases

Daewon Lee, Minjin Kim, and Kwang-Hyun Cho*

Department of Bio and Brain Engineering,
Korea Advanced Institute of Science and Technology (KAIST),
291 Daehak-ro, Yuseong-gu, Daejeon, 305-701, Republic of Korea

* To whom correspondence should be addressed: E-mail: ckh@kaist.ac.kr, Phone: +82-42-350-4325, Fax: +82-42-350-4310

I. Supplementary Methods

- S1. Biological examples of ITUD system
- S2. Development of mathematical models for ITUD system
- S3. *In silico* cell population dynamics
- S4. *In vitro* experiments

II. Supplementary Notes

Supplementary Note 1. Limitation in preparing experimental systems.

III. Supplementary Figures

Supplementary Figure S1. Density plots for ratios of sensitivities over a wide range of parameter values.

Supplementary Figure S2. Diverse shapes of the biphasic curves in ITUD system.

Supplementary Figure S3. Temporal dynamics over a wide range of parameter values with or without noise in signal.

Supplementary Figure S4. Temporal dynamics of each cell type in *in silico* analysis of cell proliferation.

Supplementary Figure S5. Gene expression and cell proliferation assay.

IV. Supplementary Tables

Supplementary Table S1. Mathematical models for SNFL, DTUD, and ITUD system.

Supplementary Table S2. A set of the nominal values for kinetic parameters

V. Supplementary Movies

Supplementary Movie S1. A representative movie of *in silico* cell proliferation dynamics without perturbation (control).

Supplementary Movie S2. A representative movie of *in silico* cell proliferation dynamics under perturbation.

Supplementary Movie S3. A representative movie of *in silico* cell migration dynamics under perturbation.

Supplementary Movie S4. A representative movie for the diffusion field of signal S .

VI. Supplementary References

I. Supplementary Methods

S1. Biological examples of ITUD system

All of the following biological evidences have been collected from literatures that report the results of biological experiments with heterogeneous backgrounds such as cell lines or experimental conditions. The schematic diagrams of the examples do not cover all the regulations, but include essential biochemical reactions we are interested in. These examples do not insist the structures or dynamics of the signaling pathways are always functional in any cell line, but suggest that the systems can operate based on the configurations presented here. To confirm the existence and functionality of the exemplified signaling pathways, extensive *in vitro* and *in vivo* experiments are required to see whether the interconnected biochemical reactions occur in chosen cell lines or animal models over various conditions.

S1.1. Skp2 in c-Myc pathway

In the example of Skp2 in c-Myc pathway, Skp2 is a transcription cofactor which forms a transcriptional complex with Myc, Miz-1 and p300 to induce RhoA transcription¹. Overexpression or knockdown of the components in the Myc-Skp2-Miz1 affected breast cancer metastasis in mouse model, and the results were positively correlated with the level of RhoA¹.

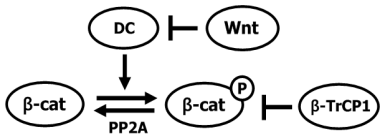
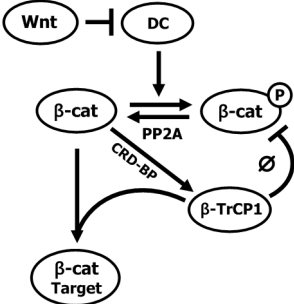
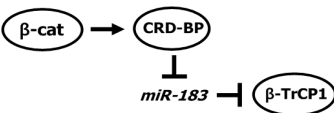

The transcriptional activation and the subsequent destruction of transcription factor through UPS has been explained with models such as “time clock” (also known as “timer”, “molecular clock”, “Ub clock”, “licensing”)²⁻⁷ or “black widow”^{3,8}. In the “time clock” model, the initial mono-ubiquitination of transcription factor is a necessary event for transcriptional activation, and the subsequent maturation of ubiquitin chain (i.e., poly-ubiquitin) promotes the proteasomal degradation of the transcription factor. Thus, the stepwise linkage of ubiquitins acts as a ‘timer’ or ‘clock’ which limits the time for a single molecule of the transcription factor to activate the gene expression. In the “black widow” model, the poly-ubiquitination and the subsequent destruction of transcription factor after recruiting general transcription machineries involving RNA polymerase II holoenzyme is a necessary process for the productive initiation of transcription. The ‘black widow’ means a female venomous spider (*transcription machineries including UPS*) who eats (*destructs*) her male partner (*transcription activator*) after mating (*formation of the transcription complex and transcriptional activation*). Although both models have some differences, they are similar in a way that ubiquitination tightly controls life-cycle of the transcription factor at the promoter.

Diagram	Regulations	
		<p>The SCF(Skp2) ubiquitin ligase complex poly-ubiquitinates c-Myc for proteasomal proteolysis ^{2,9}. Unlike other interactions between c-Myc and E3 proteins ^{10,11}, the interaction between c-Myc and Skp2 does not depend on the phosphorylation of c-Myc ⁹.</p>
		<p>c-Myc can enhance the expression of Skp2 directly ^{12,13}, or indirectly promote the interaction between c-Myc and Skp2 for the proteasomal degradation ¹⁴.</p>
		<p>Skp2 transactivates a set of c-Myc target genes. The participatory form of Skp2 in the transcriptional activation of c-Myc can be a ubiquitin ligase receptor in SCF complex for the destructive poly-ubiquitination ^{2,9}, or a cofactor without ubiquitin ligase activity ¹.</p>

S1.2. β -TrCP1 in β -catenin pathway

Human cells have two β -TrCP proteins: β -TrCP1 and β -TrCP2. Many studies reported that these β -TrCP proteins are indistinguishable in biochemical properties ¹⁵ or proteolysis of β -catenin, Wee1, I κ B, etc ¹⁶. Thus, the total amount of β -TrCP1 and β -TrCP2 in a cell that can respond to Wnt signal might be important for the proteolysis of the target proteins. In this study, however, it is assumed that β -TrCP2 does not affect the amount of total β -TrCP pool for regulating β -catenin, and it is considered as a kind of genetic redundancy ¹⁷.

The recent papers suggest that various isoforms of β -TrCP have differences in substrate specificity, subcellular localization, and expression pattern over different tissues ^{18,19}. Intriguingly, β -TrCP proteins are oppositely regulated by β -catenin/TCF signaling: β -TrCP1 is enhanced through CRD-BP which is induced by β -catenin/TCF, and β -TrCP2 is inhibited by direct binding of β -catenin on its promoter ²⁰. In addition, an opposite mRNA expression pattern of β -TrCP1 and β -TrCP2 in sperm development was also observed ²¹. It might be interesting to understand how the balance between the concentrations of β -TrCP isoforms changes the dynamics and stability of the target proteins in the future study.

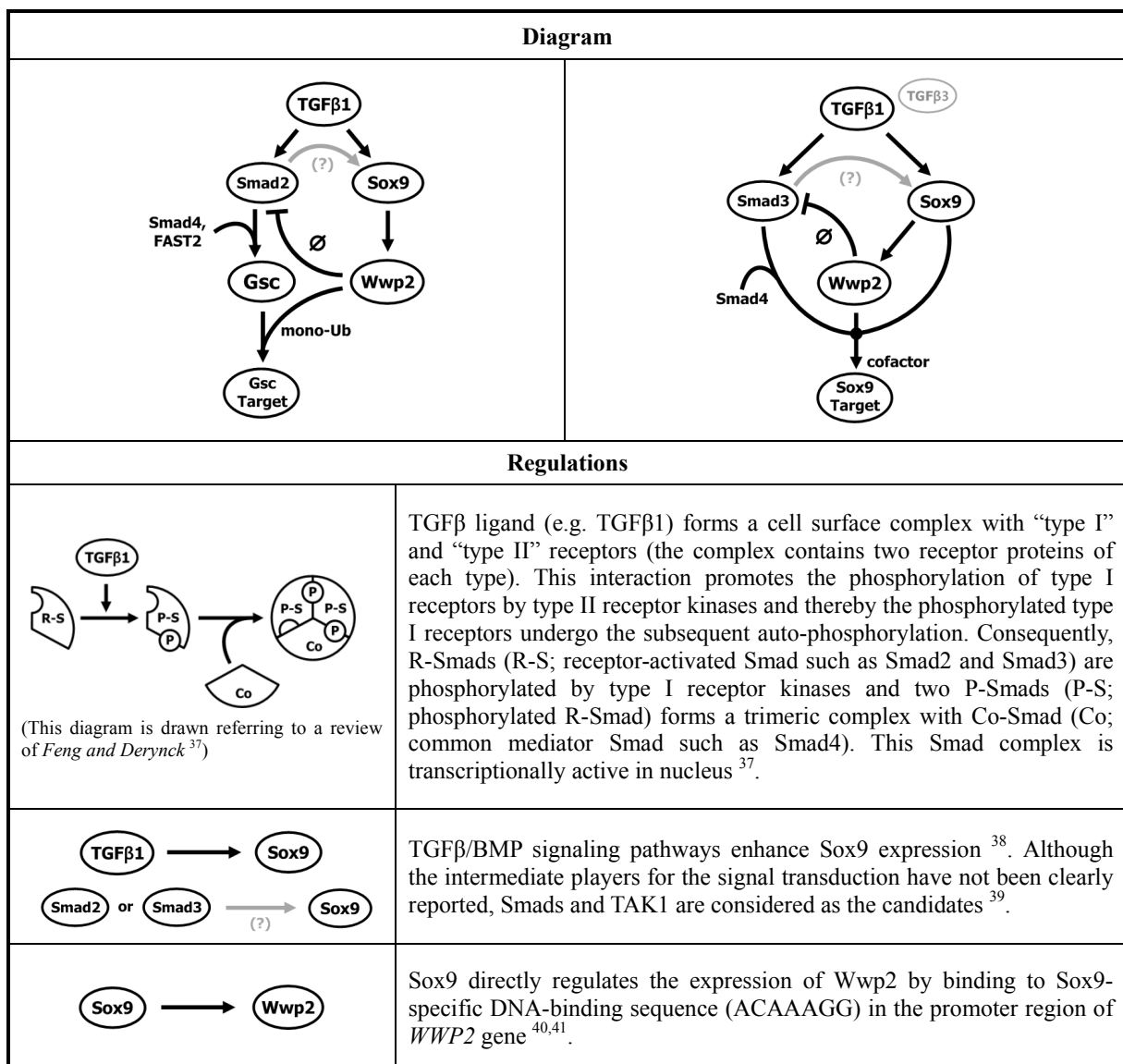
Diagram	Regulations
	 <p>In Wnt/β-catenin pathway, β-TrCP1 (also known as Fbw1a) in SCF complex binds to the phosphorylated β-catenin. The phosphorylation of β-catenin at serine residues 37 and 33 is mediated by destruction complex (DC). β-TrCP1 promotes the poly-ubiquitination of β-catenin for its 26S proteasomal degradation²². On the other hand, the phosphorylation and subsequent ubiquitination can be reversed by phosphatase (e.g. PP2A²³) and deubiquitinase (e.g. Fam²⁴), respectively.</p> <p>When Wnt signal stimulates a receptor complex of Fz and LRP5/6, the phosphorylation of β-catenin by DC is inhibited and thereby β-catenin is stabilized and accumulated in nucleus. The stabilized β-catenin in nucleus can serve as a coactivator for TCF to transactivate Wnt-responsive genes²². However, β-catenin that is phosphorylated at S37 and S33 is known as transcriptionally inactive²⁵.</p>
	 <p>Wnt/β-catenin signaling induces expression of β-TrCP1²⁶. β-catenin promotes the expression of CRD-BP²⁷ and then CRD-BP prevents β-TrCP1 mRNA from being degraded by miR-183²⁸. The stabilized β-TrCP1 plays as a negative feedback together with Axin2²⁹⁻³¹.</p>
	 <p>β-TrCP1 cooperates with p300 to up-regulate the expression of β-catenin target genes such as Cyclin D1 without ubiquitin ligase activity³². That is, β-TrCP1 can be a transcription cofactor for a set of β-catenin target genes.</p>

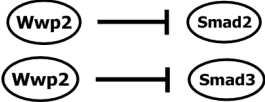
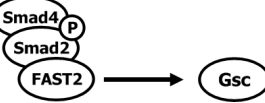
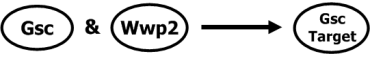
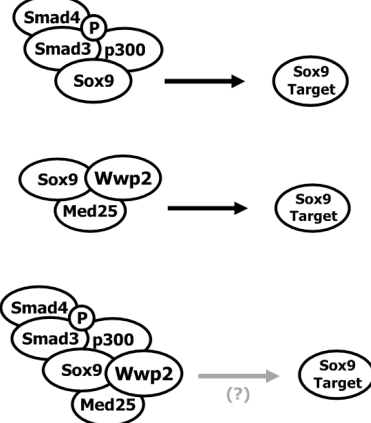
S1.3. Wwp2 in Smad2/3 pathway

In the example of TGF β /Smad pathway, Wwp2 can be a transcription factor which mono-ubiquitinates Gsc or acts as a cofactor of Sox9 for the transcriptional activation, respectively. Although both Gsc and Sox9 pathways can work together, we present them here in separated diagrams.

The biochemical regulations have been collected from biological experiments which are mainly related

to chondrogenesis, craniofacial development and palatal formation. In some studies, TGFβ3 was used rather than TGFβ1 for TGF stimulation^{33,34}. The effects of TGFβ1 and TGFβ3 on suture-derived mesenchymal cells (SMCs) from mouse posterior frontal suture were different³⁵. In contrast, TGFβ1 and TGFβ3 showed almost the same results for the induction of chondrogenesis in mesenchymal stem cells (MSCs) from human bone marrow³⁶. In this study, we do not specifically distinguish both TGFβ1 and TGFβ3 in Smad pathway.



	<p>Wwp2 is a HECT-type E3 ubiquitin ligase which has intrinsic ubiquitin ligase activity. In contrast, RING type E3s such as Skp2 and β-TrCP1 have no intrinsic ubiquitin ligase activity, but merely play a role as receptors to recognize their targets. The full-length Wwp2 (Wwp-FL) promotes UPS-dependent degradation of unstimulated or stimulated Smad2/3 (R-Smads or P-Smads) with or without TGFβ signal. However, the proteolysis of Smads by Wwp-FL is relatively slow under TGFβ signal due to the behavior of Wwp2-N. Refer to a recent study⁴² and a review⁴³ for more detailed information.</p>
	<p>TGFβ signal allows the formation of FAST2/Smad2/Smad4 complex, termed TRF (TGFβ/activin response factor). This complex directly binds to Goosecoid (Gsc) promoter through the forkhead domain of FAST2⁴⁴.</p>
	<p>Mono-ubiquitination of Gsc by Wwp2 activates the expression of Gsc target genes such as Sox6⁴⁰.</p>
	<p>Smad3 enhances the transcriptional activity of Sox9 together with p300 in a TGFβ-dependent manner. The results of Smad2, however, were not significant^{33,34}.</p> <p>Wwp2 can be a cofactor for the transcriptional activity of Sox9. Wwp2 facilitates the nuclear translocation of Sox9 and mediates the formation of transcriptional complex with Sox9 and Med25⁴¹.</p> <p>Both of Smad3/Sox9 and Sox9-Wwp2-Med25 complexes can regulate <i>Col2a1</i> gene expression. Therefore, we cannot exclude the possibility that Smad3, Sox9, Wwp2 and Med25 cooperate for the expression of <i>Col2a1</i> gene in the same transcription complex.</p>

S1.4. β -TrCP1 in Smad3 pathway

Refer to “S1.3. Wwp2 in Smad2/3 pathway” for the regulations in the canonical Smad3 pathway.

Diagram	Regulations	
		<p>The complex of Smad3 and Smad4 prevents UPS-dependent proteolysis of β-catenin⁴⁵. The stabilized β-catenin can enhance the expression of β-TrCP1 through CRD-BP (refer to S1.2. β-TrCP1 in β-catenin pathway).</p>
		<p>β-TrCP1 promotes the UPS-dependent proteolysis of Smad4⁴⁶.</p>
		<p>β-TrCP1 also promotes the UPS-dependent proteolysis of Smad3⁴⁷, but it depends on the formation of complex with Smad4^{46,48}. The interaction between Smad3 and β-TrCP1 was abolished by Smad4 gene silencing.</p>
		<p>As in the case of β-catenin, β-TrCP1 also augments the transcriptional activity of Smad3 by playing as a cofactor³².</p>

S2. Development of mathematical models for ITUD system

S2.1. Details and major assumptions

The mathematical model of ITUD system (Supplementary Table S1) is a biochemical network consisting of one negative feedback loop and AND-gated regulation for the system output (in a point of view, the structure is a feed-forward loop with a single negative feedback). Rapid enzyme-substrate reactions and relatively slow transcriptional processes comprise the negative feedback loop, in which $E3$ promotes the degradation of T and T induces the expression of $E3$. This negative feedback loop has an important role to maintain an appropriate level of T by controlling the balance between T and $E3$. Degradation of a protein can be modeled in a wide range of complexity from realistic to simplified⁴⁹⁻⁵². In this study, we have reached a trade-off, in which the UPS-dependent proteolysis of T by $E3$ includes three reactions: 1) poly-ubiquitination, 2) deubiquitination, and 3) proteasomal destruction. All these reactions are modeled based on Michaelis-Menten (MM) type kinetics^{53,54}: the ubiquitination of T promoted by $E3$ is described by Eq. S1, and deubiquitination and proteasomal destruction by Eq. S2. Briggs-Haldane (BH) kinetics⁵⁵ can also be applied, but we do not distinguish the detailed assumptions between MM and BH kinetics in this study⁵⁶.

$$f_{MM}(E, S) = k_{cat} E_{tot}(t) \frac{S(t)}{K_m + S(t)} \quad (\text{Eq. S1})$$

$$g_{MM}(S) = V_{max} \frac{S(t)}{K_m + S(t)} \quad (\text{Eq. S2})$$

The form of Eq. S1 is identical to that of “saturated degradation”⁵¹. However, the assumption stems from a different idea. While the production and accumulation of a protein incorporating the processes such as transcription, translation and post-translational modification take many minutes to hours⁵⁷, enzyme-substrate reactions such as phosphorylation, ubiquitination, deubiquitination and proteasomal degradation occur on a second timescale^{50,58-60}. Thus, it is reasonable to assume that the total amount of enzyme changes with respect to time, when MM kinetics is included in a transcriptional network on an hour timescale. In ITUD, $E3$ promotes the ubiquitination of T and, at the same time, $E3$ is transcriptionally regulated by T . So, we have chosen Eq. S1 as the kinetics model to reflect the dynamic pool of $E3$ proteins active for proteolysis of T . The rest of enzyme-substrate reactions are modeled with the typical MM equation (Eq. S2), because the levels of the regulators such as deubiquitinases (deubiquitinating enzymes; DUBs) or proteasomes are assumed to be constant.

One might ask why phosphorylation is omitted in the interaction between T and $E3$. The phosphorylation of target proteins is important for a family of E3 ligases such as F-box proteins to recognize the target proteins. A representative example is the case of β -catenin and β -TrCP1. β -catenin

has an amino acid sequence, “DSGIHS”, which is called “degron”¹⁶. The two serine residues in the degron sequence need to be phosphorylated by the destruction complex (DC) for the interaction between β -catenin and β -TrCP. If an APC mutation occurs and thereby DC fails to form appropriately, β -catenin cannot be phosphorylated⁶¹. The abnormal stabilization of β -catenin due to the DC breakdown and loss of the phosphorylation has been seriously investigated in colorectal carcinogenesis⁶². In this study, however, we consider the phosphorylation as a signal to specify a target transcription factor among many substrates to undergo UPS-dependent proteolysis (cf. F-Box proteins usually have various targets^{63,64}). As T is only one target for degradation in ITUD, we did not include the phosphorylation-dependent substrate recognition (we discuss the regulatory role of phosphorylation in the biphasic response of ITUD in the main text).

The participatory form of $E3$ in transcription can be a transcription cofactor without ubiquitin ligase activity, or a ubiquitin ligase for mono-ubiquitination and destructive poly-ubiquitination of T at the promoter of P . However, we do not distinguish the mode of $E3$ in the transcription process. We assumed that a possible degradation of T by $E3$ at the promoter of P in ITUD is relatively weak and thus it is negligible. By contrast, the proteolysis of T outside the promoter is independent of the transcription cycle⁶⁵ and therefore it may more actively affect the stability of T . Although UPS-mediated proteolysis linked to transcriptional activation is capable of affecting the stability of transcription factor^{66,67}, the above assumption is adopted in this study. Hence, we have employed multiplied Hill equations (Eq. S3) to describe the transcriptional regulation of P by T and $E3$. This AND-gated Hill function was used for modeling a coherent feed-forward loop⁶⁸.

$$f_P(T, E3) = \left(\frac{[T]^{n_1}}{K_1^{n_1} + [T]^{n_1}} \right) \left(\frac{[E3]^{n_2}}{K_2^{n_2} + [E3]^{n_2}} \right) \quad (\text{Eq. S3})$$

$$g_P(T, E3) = \frac{T^{n_1} (K_2^{n_2} + E3^{n_2})}{K_1^{n_1} K_2^{n_2} + T^{n_1} (K_2^{n_2} + E3^{n_2})} \quad (\text{Eq. S4})$$

An alternative to the AND-gated Hill function (Eq. S3) is a model termed “E3-relaxation model” (Eq. S4, see “**S2.2. Derivation of E3-relaxation model**”). In the E3-relaxation model, T has a basal transcriptional activity for P regardless of $E3$, and $E3$ ‘relaxes’ the threshold for T to achieve the active expression of P . However, this model has limitations to reflect real phenomena. Let’s consider ‘knockout’ and ‘overexpression’ of T or $E3$ in both AND-gated Hill function and E3-relaxation function. When T is knocked out ($T \rightarrow 0$), these two functions have zeros. However, when T is overexpressed ($T \rightarrow \infty$), the AND-gated Hill function converges to a typical Hill function which depends on $E3$ only. In contrast, the E3-relaxation function merely converges to 1, which means that T can achieve the maximal production of P without $E3$. In the case of $E3$ knockout condition ($E3 \rightarrow 0$), the AND-gated Hill function has zero, while the E3-relaxation model converges to a typical Hill function of T . When $E3$ is overexpressed ($E3 \rightarrow \infty$), the E3-relaxation function converges to 1 (the maximal production), while the AND-gated Hill function becomes a typical Hill function of T . This means that the expression of P in the

E3-relaxion model can reach its maximal activity, irrespective of T . All the above cases are summarized as follows:

Condition \ Type	AND-gated Hill function	E3-relaxation function
$T \rightarrow 0$	0	0
$T \rightarrow \infty$	$\frac{[E3]^{n_2}}{K_2^{n_2} + [E3]^{n_2}}$	1*
$E3 \rightarrow 0$	0	$\frac{[T]^{n_1}}{K_1^{n_1} + [T]^{n_1}}$
$E3 \rightarrow \infty$	$\frac{[T]^{n_1}}{K_1^{n_1} + [T]^{n_1}}$	1*

※ The problematic results are denoted by asterisk (*).

The experimental reports, however, demonstrate $E3$ and T reciprocally affect each other under the overexpression condition ^{1,2,9,32}. Therefore, we suggest the AND-gated Hill function is more plausible for ITUD system rather than the E3-relaxation model.

The followings are the rest of assumptions to develop the mathematical models:

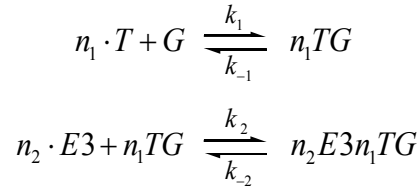
1. We confine the temporal dynamics of ITUD to monotonic behavior, and set the steady-state level of P as the most important measure for analyzing the system. Therefore, we rule out other properties of biological negative feedback loops such as oscillation ^{52,69}, which is not within the scope of this study. Furthermore, the derivative of incoherent feed-forward loop (I-FFL) exemplified by Smad/Wwp2 is not profoundly taken into account, because simple monotonic dynamics of I-FFL is almost the same with that of negative feedback loop except that signal in I-FFL is conveyed directly from S to $E3$, not through T . On the other hand, Smad/Wwp2 pathway might also have negative feedback loops rather than I-FFL, if Sox9 is a downstream factor of Smad2/3 ³⁹ (see “**S1.3. Wwp2 in Smad2/3 pathway**”).
2. The UPS-dependent degradation of T can occur in any place, including both cytoplasm and nucleus. Thus, the state variables for each protein are not divided according to subcellular localization.
3. We suppose that there is no competition for the pool of $E3$ between the degradation of T and the transcriptional activation of T at the promoter of P in ITUD. It is possible that the pool of $E3$ protein is limited in a cell ⁷⁰, and then the mode of a $E3$ protein can be decided according to binding affinities or extra regulations on $E3$ protein ^{71,72}. However, the effects of the competition are not considered in this study.
4. It is assumed that $E3$ does not participate in the transcriptional activation of itself.

5. The values of parameter set are determined to explain the concepts and properties of the generalized system⁷³⁻⁷⁷. We did not intend to store biochemical information in a set of parameters, or to capture biological features of real systems⁷⁸⁻⁸⁰. The values of parameter set we used for analysis are presented in Supplementary Table S2.

S2.2. Derivation of E3-relaxation model

The following is the derivation of E3-relaxation model, which is based on a comprehensible introduction for kinetics of gene regulation⁸¹. The E3-relaxation model explains how *E3* ubiquitin ligase cooperates with *T* at the promoter of *P* (refer to the Supplementary Table S1 for the abbreviations: *T*, *E3*, and *P*). Transcription factor (abbr., *T*) binds to the promoter of *P* (abbr., *G*) and then it forms a transcription complex (abbr., *TG*). If n_1 molecules of *T* are necessary for the interaction with *G*, they form a transcription complex (abbr., n_1TG). This transcription complex involving general transcriptional machineries can promote the expression of *P*.

On the other hand, *E3* cannot form a transcription complex with *G* without *T*. The transcriptional behavior of *E3* depends on *T*. It is shown that *E3* requires *T* for the transcriptional activation in the *T* null cells (Myc was necessary for the transcriptional effects of Skp2 on Myc target genes in Myc knockout cells⁹). Like the n_1 molecules of *T*, the n_2 molecules of *E3* interact with the *T*-bound promoter and thereby they form a transcription complex, n_2E3n_1TG . This n_2E3n_1TG complex is more active than n_1TG complex for the production of *P*. The binding kinetics of *T* and *E3* is summarized as follows:



As in the derivation of the Hill equation⁸², it is assumed that the formation of the complex rapidly reaches equilibrium. Thus, we can obtain equations as follows:

$$[n_1TG] = \frac{k_1}{k_{-1}} \cdot [T]^{n_1} \cdot [G] = \frac{1}{K_{d1}} \cdot [T]^{n_1} \cdot [G] = \frac{1}{K_1^{n_1}} \cdot [T]^{n_1} \cdot [G] \quad (\text{Eq. S5})$$

$$[n_2E3n_1TG] = \frac{k_2}{k_{-2}} \cdot [n_1TG] \cdot [E3]^{n_2} = \frac{1}{K_{d2}} \cdot [n_1TG] \cdot [E3]^{n_2} = \frac{1}{K_1^{n_1}} \cdot \frac{1}{K_2^{n_2}} \cdot [T]^{n_1} \cdot [E3]^{n_2} \cdot [G] \quad (\text{Eq. S6})$$

The k_i and $k_{.i}$ are the kinetic parameters for forward and backward reactions, respectively, and the K_{d1} and K_{d2} represent dissociation constants. Now, we can get the proportion of the gene states that are transcriptionally active over all the states of the gene by substituting Eq. S5 and Eq. S6 into Eq. S7 and eliminating the state variable of G . The arrangement of the equation is:

$$g_p(T, E3) = \frac{\text{Gene states active for transcription}}{\text{All states of the gene}}$$

$$= \frac{[n_1TG] + [n_2E3n_1TG]}{[G] + [n_1TG] + [n_2E3n_1TG]} \quad (\text{Eq. S7})$$

$$= \frac{\frac{1}{K_1^{n_1}} \cdot [T]^{n_1} \cdot [G] + \frac{1}{K_1^{n_1}} \cdot \frac{1}{K_2^{n_2}} \cdot [T]^{n_1} \cdot [E3]^{n_2} \cdot [G]}{[G] + \frac{1}{K_1^{n_1}} \cdot [T]^{n_1} \cdot [G] + \frac{1}{K_1^{n_1}} \cdot \frac{1}{K_2^{n_2}} \cdot [T]^{n_1} \cdot [E3]^{n_2} \cdot [G]}$$

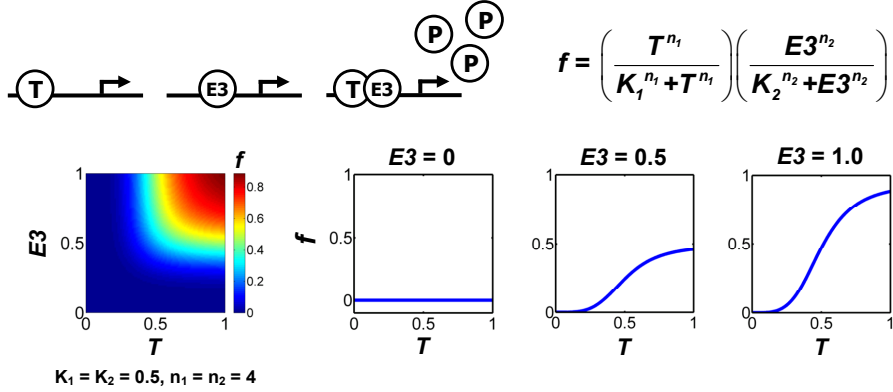
$$= \frac{\frac{1}{K_1^{n_1}} \cdot [T]^{n_1} + \frac{1}{K_1^{n_1}} \cdot \frac{1}{K_2^{n_2}} \cdot [T]^{n_1} \cdot [E3]^{n_2}}{1 + \frac{1}{K_1^{n_1}} \cdot [T]^{n_1} + \frac{1}{K_1^{n_1}} \cdot \frac{1}{K_2^{n_2}} \cdot [T]^{n_1} \cdot [E3]^{n_2}}$$

$$= \frac{[T]^{n_1} (K_2^{n_2} + [E3]^{n_2})}{K_1^{n_1} K_2^{n_2} + [T]^{n_1} (K_2^{n_2} + [E3]^{n_2})} \quad (\text{Eq. S8})$$

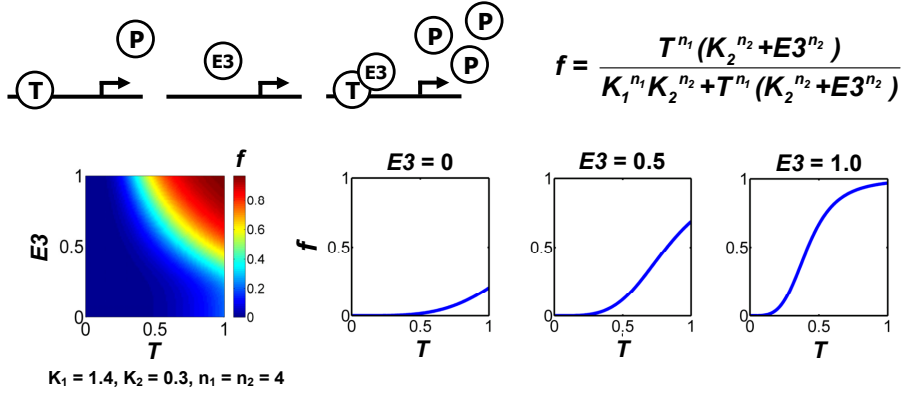
$$= \frac{[T]^{n_1}}{\left(\frac{K_1^{n_1}}{1 + \left(\frac{[E3]}{K_2} \right)^{n_2}} \right) + [T]^{n_1}} \quad (\text{Eq. S9})$$

The K_1 and K_2 stand for the half-maximal occupancies, and the n_1 and n_2 are the Hill coefficients which describe the cooperativity or the characteristics of steepness⁸¹⁻⁸³. Eq. S8 is the final form of the E3-relaxation model. To understand why it is named ‘‘E3-relaxation’’, we need to divide both numerator and denominator in Eq. S8 by $(K_2^{n_2} + [E3]^{n_2})$. The result is Eq. S9, which is similar to the typical Hill equation. As $E3$ increases, this function behaves as if the half-maximal occupancy in the typical Hill function decreases (cf. $K_A = K_i^{n_i} / (1 + ([E3]/K_2)^{n_2})$). In other words, $E3$ ‘relaxes’ the threshold which T has to exceed for the transcriptional activation. The following figure shows how E3-relaxation model works in comparison to the AND-gated Hill function.

1. AND



2. E3-relaxation



The E3-relaxation model allows a leakage from the transcription of T , when there is no $E3$. In contrast, the AND-gated Hill function has zero value if there is no $E3$. The 2D color plots for the function values with respect to T and $E3$ are roughly similar, although the shapes of the plots are slightly different between the two functions. The most noticeable difference between the AND-gated Hill function and E3-relaxation model is discussed in the previous section, “**S2.1. Details and major assumptions.**”

S2.3. Mathematically controlled comparison

M. A. Savageau and researchers have established a method called “*Mathematically Controlled Comparison (MCC)*”^{77,84-86}. MCC characterizes the inherent properties of a given system by comparing it with alternative systems which have slightly different components or relationships from the original system (or reference system)⁸⁵. To apply this method, we need to satisfy some requirements: 1) *formulation of alternative systems*, 2) *internal equivalence* and 3) *external equivalence*. These requirements help to avoid a wrong conclusion from the accidental differences between the compared

systems.

In this study, the alternative systems are SNFL and DTUD (Fig. S2 and Supplementary Table S1). All the three systems share a negative feedback loop. The difference among these systems is the form of transcriptional regulation for the system output, P . In SNFL, P is affected by only T . In DTUD, the proteolysis and transcriptional activation are promoted by different components. That is, an additional node, I , participates in the transcriptional activation and $E3$ only facilitates the UPS-dependent degradation of T in DTUD.

The internal equivalence means the identical parts among the compared systems need to be the same. It is satisfied by assigning the same values to the common parameters in the negative feedback loop (Supplementary Table S2). On the other hand, the external equivalence controls the unique parts of each system to have almost the same results among the compared systems as long as possible. This requirement reduces the accidental differences by constraining degrees of freedom⁸⁵. In this study, the mathematical form of the transactivation function for the production of P and the related parameters are ‘controlled’ to have almost the same results when a set of kinetic parameters is given. First, SNFL also has the AND-gated Hill function as the other systems do. This function, however, has a single independent variable, T , while the other systems have two independent variables. Second, the unique parameter values of the alternative systems should be determined to obtain the results that are almost the same with that of ITUD system. As the system output is the steady-state level of P (P_{ss}), we can achieve the external equivalence by equating the mathematical expressions for the steady-state level of P as follows:

$$\frac{\beta_P}{\alpha_P} + \frac{\beta_{TE3P}}{\alpha_P} \cdot \left(\frac{[T_{ss}]^{n_{TP}}}{K_{TP}^{n_{TP}} + [T_{ss}]^{n_{TP}}} \right) \left(\frac{[E3_{ss}]^{n_{E3P}}}{K_{E3P}^{n_{E3P}} + [E3_{ss}]^{n_{E3P}}} \right) = \frac{\beta_P}{\alpha_P} + \frac{\beta_{TP}}{\alpha_P} \cdot \left(\frac{[T_{ss}]^{n_{TP}}}{K_{TP}^{n_{TP}} + [T_{ss}]^{n_{TP}}} \right) \left(\frac{[T_{ss}]^{n_{TP2}}}{K_{TP2}^{n_{TP2}} + [T_{ss}]^{n_{TP2}}} \right)$$

The left expression is the steady-state level of P in ITUD and the right one is that of SNFL. The T_{ss} and $E3_{ss}$ represent the steady-state level of T and $E3$, respectively. For simplicity, we set $\beta_{TE3P} = \beta_{TP}$ and $n_{E3P} = n_{TP2}$, and subsequently we can obtain the following equations derived by removing the same terms in the above equation.

$$\left(\frac{[E3_{ss}]^{n_{E3P}}}{K_{E3P}^{n_{E3P}} + [E3_{ss}]^{n_{E3P}}} \right) = \left(\frac{[T_{ss}]^{n_{TP2}}}{K_{TP2}^{n_{TP2}} + [T_{ss}]^{n_{TP2}}} \right)$$

$$\frac{[E3_{ss}]^{n_{E3P}} K_{TP2}^{n_{TP2}} - [T_{ss}]^{n_{TP2}} K_{E3P}^{n_{E3P}}}{(K_{E3P}^{n_{E3P}} + [E3_{ss}]^{n_{E3P}})(K_{TP2}^{n_{TP2}} + [T_{ss}]^{n_{TP2}})} = 0 \quad (\text{Eq. S10})$$

This equation is the *constraint equation*⁸⁵ in this study, which is used to determine the unique values of the alternative systems. It makes the outputs of the compared systems have almost the same values as long as possible. The only unique parameter, K_{TP2} , can be determined by solving Eq. S10 as follows:

$$K_{TP2}^{n_{TP2}} = \frac{[T_{ss}]^{n_{TP2}} K_{E3P}^{n_{E3P}}}{[E3_{ss}]^{n_{E3P}}}$$

$$K_{TP2} = K_{E3P} \frac{[T_{ss}]}{[E3_{ss}]}$$

$$(\because n_{E3P} = n_{TP2}, K_{TP2} > 0)$$
(Eq. S11)

The T_{ss} and $E3_{ss}$ in ITUD are the same with those of SNFL and DTUD since they share the identical negative feedback loop. Given a set of parameters in ITUD (Supplementary Table S2), the constrained value of K_{TP2} is 0.5166 (we obtained $T_{ss} = 0.9772$ and $E3_{ss} = 0.9459$ from the numerical solution of the steady-state levels, when S was 1.0). However, using the same value for K_{E3P} and K_{TP2} also gives us a good estimate. When we have $K_{E3P} = K_{TP2} = 0.5$, the ratio of the two P_{ss} (i.e., P_{ss_SNFL}/P_{ss_ITUD}) is 1.0088. This means the difference between the outputs of ITUD and SNFL using $K_{E3P} = K_{TP2} = 0.5$ is within 1%.

Indeed, the above constraint equation does not fully satisfy the criteria in MCC, because it does not include the constraint equation for DTUD system. In order to mathematically control DTUD, we should set both of the ODE of I and the related parameters in DTUD being identical to those of $E3$ in ITUD (Supplementary Table S1 and S2). However, this constraint results in that the whole parts of DTUD becomes identical to that of ITUD, as I becomes identical to $E3$. Therefore, we have a ‘semi-constraint’ equation for DTUD system, in which all the parameters for the transcriptional regulation of P by I are equal to those of $E3$ in ITUD. The following is a summary of the conditions for MCC in this study.

Mathematically controlled comparison (MCC)		
Compared systems	Reference	ITUD
	Alternative	SNFL and DTUD
Internal equivalence	Common parameters are assigned the same values (Supplementary Table S2).	
External equivalence	System property	The steady state level of system output, P
	Constraint equation	$\left(\frac{[E3_{ss}]^{n_{E3P}}}{K_{E3P}^{n_{E3P}} + [E3_{ss}]^{n_{E3P}}} \right) = \left(\frac{[T_{ss}]^{n_{TP2}}}{K_{TP2}^{n_{TP2}} + [T_{ss}]^{n_{TP2}}} \right)$ $\rightarrow K_{TP2} = K_{E3P} \frac{[T_{ss}]}{[E3_{ss}]}$

S3. *In silico* cell population dynamics

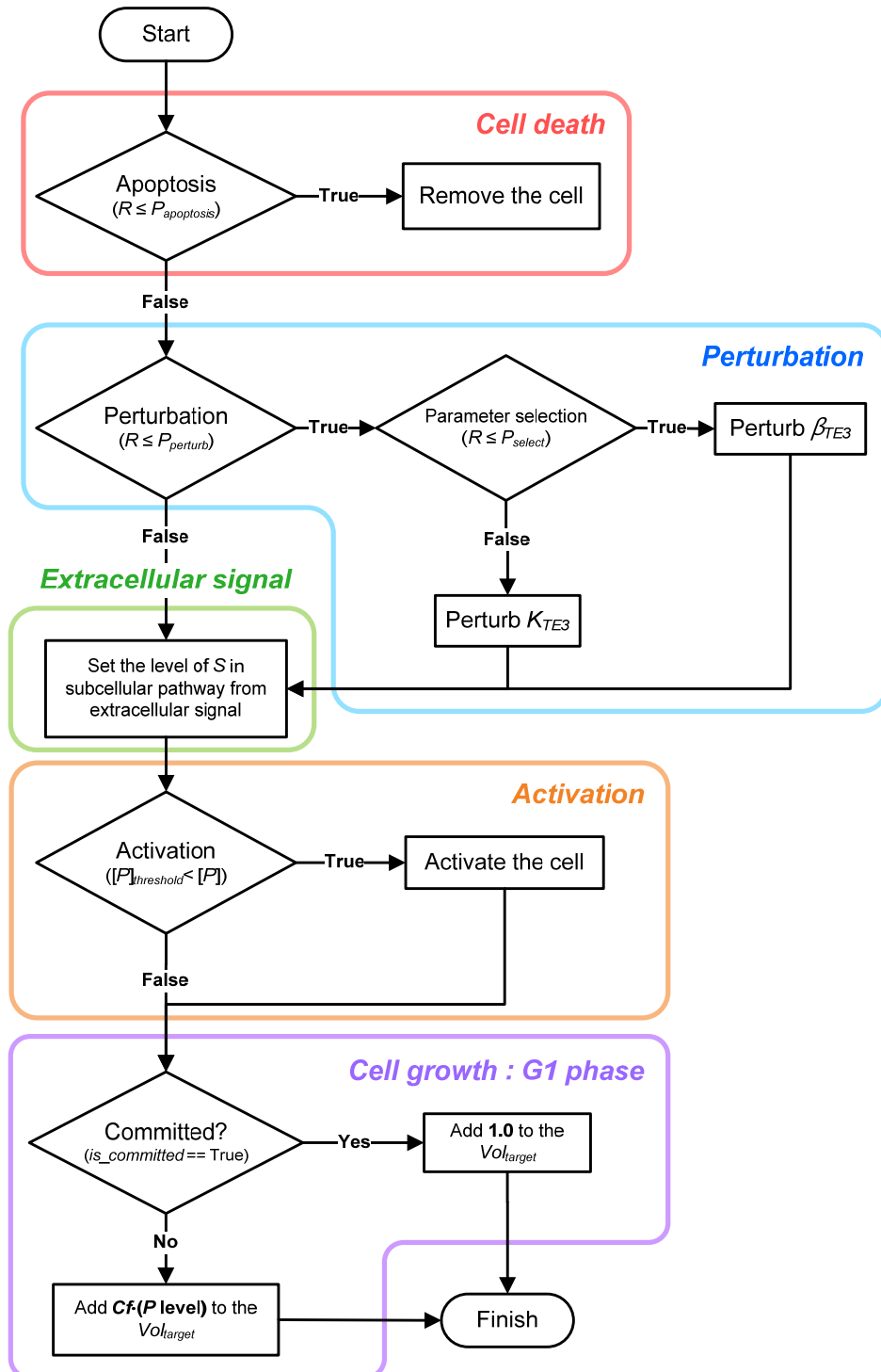
Cell population dynamics in this study was implemented on CompuCell3D (CC3D), which is one of the state-of-the-art multiscale modeling platforms ⁸⁷. The cell population model of CC3D is based on the Cellular Potts Model (CPM) ⁸⁸. We developed a simple cell cycle model and integrated it with a subcellular pathway model such as SNFL, DTUD and ITUD. The ordinary differential equations of subcellular pathway models were numerically solved by Bionetsolver ⁸⁹ in CC3D.

S3.1. Cell proliferation

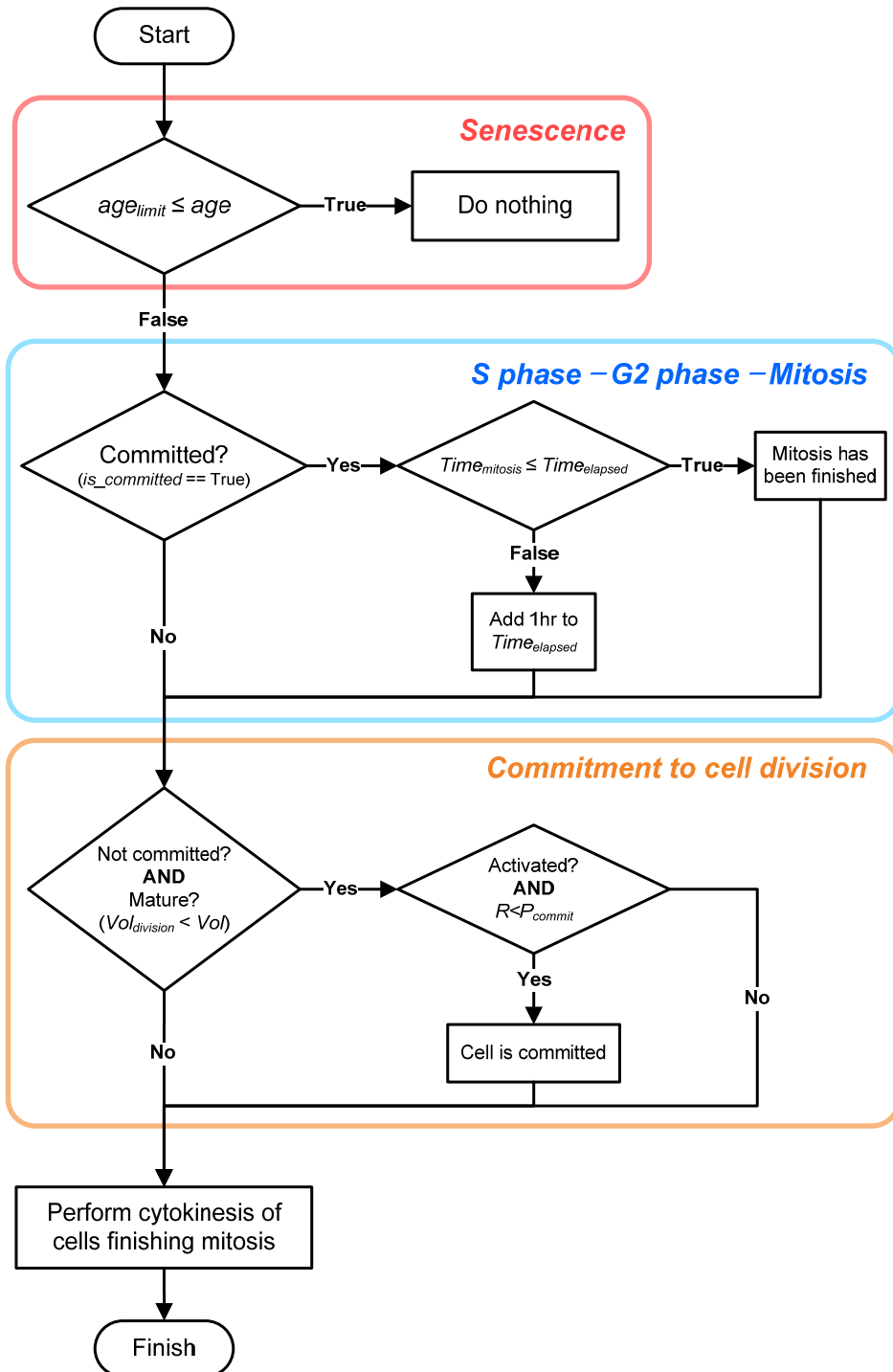
S3.1.1. Cell cycle model

Proliferation of metazoan cells is thought to depend on various mechanisms, by which cell growth and cell cycle are controlled. In the simulation of this study, cell cycle progression for division is promoted by cell growth ⁹⁰. A cell commits to division, when cell growth is stimulated by proliferation signal and its size (cell volume) reaches a certain point (cf. in contrast, there is a report suggesting that cell division can be independent of cell size ⁹¹). Our cell cycle model consists of two modules: 1) subcellular pathway and 2) mitosis. These modules are implemented as Python “Steppable”s of CC3D, which are executed every simulation step. The flow diagrams of the cell cycle model are presented as the following figures (the related parameters and variables are also provided in the following tables).

< A flow diagram for the **subcellular pathway** module >



<A flow diagram for the **mitosis** module>



<Parameters>

Parameter	Value	Unit	Explanation
Subcellular pathway module			
$P_{apoptosis}$	0.001	-	Probability that apoptosis occurs.
$P_{perturb}$	0.001	-	Probability that a cell receives the perturbation.
P_{select}	0.5	-	Probability that a parameter between β_{TE3} and K_{TE3} is selected to be perturbed.
$[P]_{threshold}$	0.5	[level]	Threshold level of P ; A cell is activated when the level of P in the subcellular pathway exceeds this threshold.
Vol_{limit}	55	VU_CC3D*	Threshold volume; A cell can start cell division when its volume exceeds this threshold.
Cf	1.0	VU_CC3D·[level] ⁻¹	Converting factor; This parameter determines how much the level of P affects cell growth rate.
Mitosis module			
P_{commit}	0.5	-	Probability that a cell is committed to cell division.
age_{limit}	40	the number of cell divisions	Limitation for cell division; A cell cannot divide anymore after age_{limit} cell divisions (40 divisions in this case).
$Time_{mitosis}$	24	hour	Time a cell takes to go through S - G2 - Mitosis ; Cell cycle time of actively proliferating human cells is normally about 24 hours, which usually includes G1 phase. However, we separated G1 phase from the period time for stochastic effects caused by the extracellular activating signal, and merely defined this time as 24 hours.
$Vol_{division}$	50	VU_CC3D	Threshold volume; A cell can start cell division when its target volume exceeds this threshold.

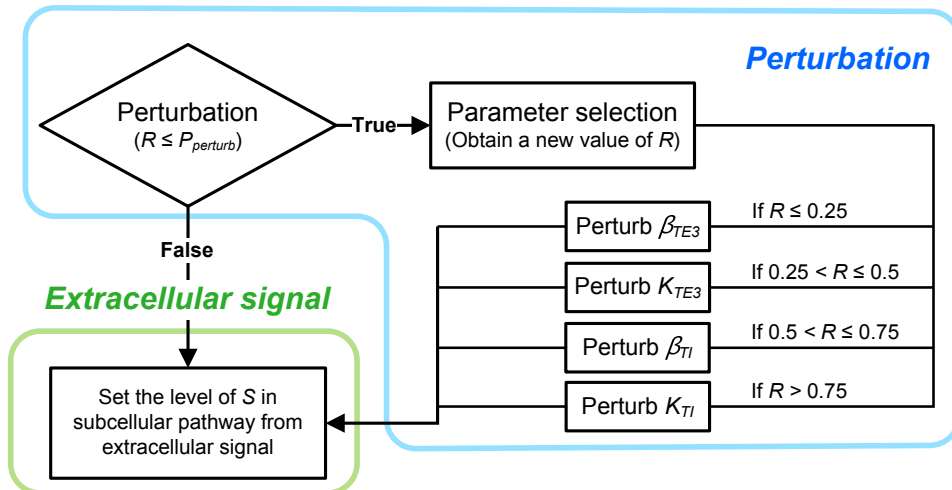
* VU_CC3D : volume unit in CompuCell3D

<Variables>

Variable	Unit	Explanation
R	-	A random variable uniformly distributed between 0 and 1.
$[P]$	[level]	The level of P in subcellular pathways such as SNFL, DTUD, and ITUD.
age	the number of cell divisions	The number of divisions a cell has finished until now.
$Time_{elapsed}$	hour	Time a cell has spent since it is committed to cell division.
Vol	VU_CC3D	Current volume of a cell, defined by CompuCell3D
Vol_{target}	VU_CC3D	Target volume of a cell, defined by CompuCell3D

The subcellular pathway module actually deals with various tasks related to cellular physiology. It includes apoptosis, subcellular perturbation, signal stimulation, cellular activation and cell growth. Apoptosis occurs in every cell with a certain probability ($P_{apoptosis}$). The apoptotic cell is removed from the simulation space. In the perturbation condition, cells undergo the perturbation of the critical determinants (i.e., the kinetic parameters for the regulation of $E3$ by T ; β_{TE3} and K_{TE3}). Perturbation also occurs with a probability ($P_{perturb}$) as apoptosis does. It was implemented in a way that one of the parameter values between β_{TE3} and K_{TE3} is randomly changed for the downregulation of $E3$ (i.e., 10~50% decrease in β_{TE3} and 10~50% increase in K_{TE3}). The perturbed cells might undergo another perturbation. So, β_{TE3} or K_{TE3} can be changed multiple times in a single cell. In DTUD-BE, one of the four parameters, β_{TE3} , K_{TE3} , β_{TI} and K_{TI} , is selected for the perturbation, as follows:

< A flow diagram for the perturbation process in DTUD-BE >



Stromal cells secrete an extracellular signal, which represents the proliferation signal in the simulation. This extracellular signal should be converted to the subcellular signal S . This process can be implemented by calling Python functions of Bionetsolver. Cells are activated when the level of P exceeds a defined threshold ($[P]_{threshold}$). This activation allows fully grown cells to be committed to cell division. Cell growth is affected by the level of P , which is the output of a subcellular pathway such as ITUD. This is implemented by multiplying the level of P with a converting factor (Cf) and then adding it to the target volume (Vol_{target}) of the cell. The committed cell, however, is not affected by the P level and its volume is maintained by the maximum growth rate.

Mitosis module incorporates the processes of cell division. It also involves senescence, S-G2-M phases, and the commitment to cell division ('commitment' is only used for cell division in this study, not for cell differentiation). We considered cellular senescence which restricts the division of a cell whose

division number exceeds a certain number of divisions (age_{limit}). To reflect the time a cell spends on S-G2-M phases, a time between the commitment and cytokinesis was defined ($Time_{mitosis}$) in the simulation. This condition also controls the proliferation rate of the cell population. The commitment to cell division is processed in mitosis module. Specifically, the volume of a cell is checked to see whether it is greater than a threshold volume ($Vol_{division}$) and the commitment occurs randomly with a probability (P_{commit}).

All types of cells except stromal cell comply with the above cell cycle model. Taking advantage of artificial properties in computational modeling, we confined the role of stromal cells to secreting extracellular signal. They do not have a subcellular pathway, perform cell division, and receive the perturbation. The growth of stromal cells is merely maintained by adding **0.05** to their target volumes every hour.

S3.1.2. Time integration

When integrating a subcellular pathway model with a cell model, the integration of time scales is one of the important issues in multiscale modeling. In the proliferation simulation, we assumed that 1 Monte Carlo Step (MCS) of CC3D corresponds to 1 hour in a subcellular pathway. The following Python code shows how the integration is implemented via Bionetsolver.

```
sbmlModelName = "ITUDModel" # name of model
sbmlModelKey = "ITUD" # designation
sbmlModelPath = "Simulation/ITUD.sbml" # file location
timeStepOfIntegration = 1.0 # 1 hour
bionetAPI.loadSBMLModel( sbmlModelName, \
                          sbmlModelPath, \
                          sbmlModelKey, \
                          timeStepOfIntegration )
```

S3.1.3. Diffusion equation

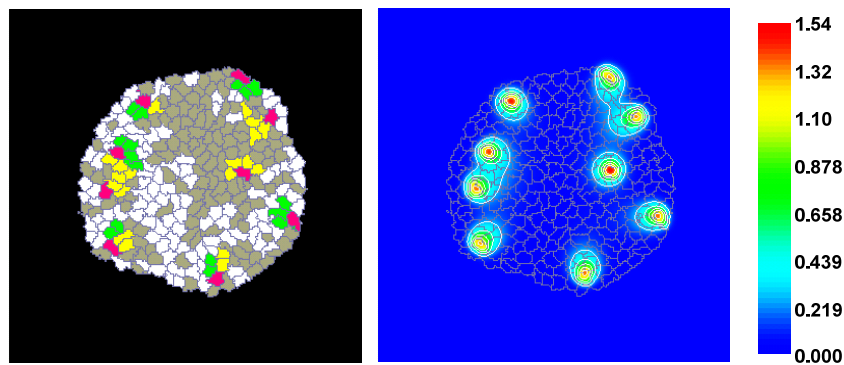
The diffusion of extracellular signal secreted by stromal cell was modeled with the following diffusion equation.

$$\frac{\partial S}{\partial t} = D_s \nabla^2 S - k_s S + p_s$$

Parameter	Value in CC3D	Value in real space	Explanation
D_s	0.25 pixel ² ·MCS ⁻¹	$2.78 \times 10^{-16} \text{ m}^2 \cdot \text{s}^{-1}$	Diffusion coefficient
k_s	0.01 MCS ⁻¹	$2.78 \times 10^{-6} \text{ m}^2 \cdot \text{s}^{-1}$	Decay/degradation rate
p_s	0.05 [level]·MCS ⁻¹	$1.39 \times 10^{-5} \text{ [level]} \cdot \text{s}^{-1}$	Production rate

※ The length of 1 pixel in the simulation space corresponds to 2 μm.

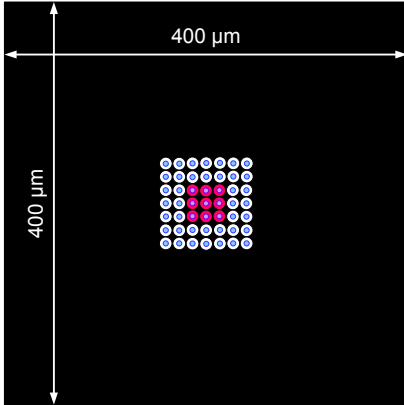
<A snapshot of the diffusion of extracellular signal>



The parameters of the diffusion equation were chosen to implement a phenomenon that secreted signal molecules (e.g., growth factors or mitogens) remain locally around the stromal cells. This attenuated diffusion of signal molecules can be attributed to the interaction between signal molecules and extracellular matrix (ECM) ⁹².

S3.1.4. Simulation settings

The initial cell population consists of 9 stromal cells surrounded by 40 normal cells (i.e., total 7×7 cells) at the center of $400 \times 400 \mu\text{m}^2$ space. The rest of parameters for CC3D simulation is summarized as follows.



Parameter	Value
Steps	10000
Temperature	5.0
Neighbor order	2
Contact energy	All the contact energy is 3 except that the energy between Mediums is 0 .
Initial target volume	25
Lambda volume	1.0

S3.2. Cell migration

S3.2.1. Chemotaxis

The *in silico* cell migration is driven by chemotaxis⁹³. It is assumed that only active cells can be attracted closely to stromal cells. Thus, active cell types (normal or perturbed) are permitted for chemotaxis. When a cell is activated, its cell adhesion strength is weakened for the facilitated movement. The lambda value we used for chemotaxis in CC3D is **5**. Morphological change of a migrating cell is not considered in this study.

S3.2.2. Cell cycle model

To confine this simulation to cell migration, we manipulated cells not to divide. Thus, cells do not have the mitosis module. The subcellular pathway module used in the proliferation simulation was also employed here, but the cell growth was different. All cells have fixed growth rates (stromal cell: **0.05** and the other cell types: **0.1**).

In the migration simulation, we varied the probability of perturbation. The following table shows the

values for three probabilities: P1, P2, and P3.

$P_{perturb}$	Value
P1	0.0001
P2	0.001
P3	0.01

P3 is the probability that represents the harshest condition. As time integration in this simulation is different from that of the proliferation simulation (i.e., 1 MCS = 1 hour), the value of P2 is actually higher than $P_{perturb}$ of the proliferation simulation. It is decided every 0.3 minutes whether perturbation occurs or not in the migration simulation. Therefore, the probability that the perturbation of P2 occurs once during an hour is about 0.164 (i.e., $\binom{200}{1}(0.001)^1(0.999)^{199} \approx 0.16389$). In comparison, the perturbation probability per hour in the proliferation simulation (i.e., $P_{perturb}$) is 0.001.

S3.2.3. Time integration

In the migration simulation, we assumed 1 MCS of CC3D corresponds to 0.3 minutes (0.005 hours) in a subcellular pathway.

S3.2.4. Diffusion equation

The diffusion equation used here is the same with that of the proliferation simulation, but parameter values are different as follows.

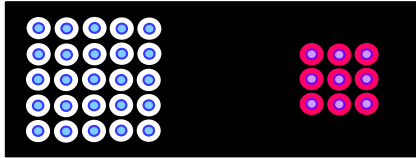
Parameter	Value in CC3D	Value in real space	Explanation
D_s	4.0 pixel ² ·MCS ⁻¹	$4.44 \times 10^{-15} \text{ m}^2 \cdot \text{s}^{-1}$	Diffusion coefficient
k_s	0.005 MCS ⁻¹	$1.39 \times 10^{-6} \text{ m}^2 \cdot \text{s}^{-1}$	Decay/degradation rate
p_s	0.05 [level] · MCS ⁻¹	$1.39 \times 10^{-5} \text{ [level]} \cdot \text{s}^{-1}$	Production rate

※ The length of 1 pixel in the simulation space corresponds to 2 μm .

S3.2.5. Simulation settings

The initial cell population consists of 25 normal cells on the left side and 9 stromal cells on the right side

in the $200 \times 80 \mu\text{m}^2$ space. The rest of parameters for CC3D simulation is summarized as follows.



Parameter	Value
Steps	10000
Temperature	5.0
Neighbor order	2
Initial target volume	25
Lambda volume	1.0

To implement the diminished cell adhesion of migrating cells at active state, we configured the contact energies in CC3D as follows.

Interaction		Value
Type1	Type2	
Homotypic interaction		
<i>Medium</i>	<i>Medium</i>	0
<i>Normal</i>	<i>Normal</i>	3
<i>Active normal</i>	<i>Active normal</i>	15
<i>Perturbed</i>	<i>Perturbed</i>	3
<i>Active perturbed</i>	<i>Active perturbed</i>	15
<i>Stromal</i>	<i>Stromal</i>	3
Cell vs. Medium		
<i>Normal</i>	<i>Medium</i>	3
<i>Active normal</i>	<i>Medium</i>	
<i>Perturbed</i>	<i>Medium</i>	
<i>Active perturbed</i>	<i>Medium</i>	
<i>Stromal</i>	<i>Medium</i>	
Heterotypic interaction		
<i>Stromal</i>	<i>Normal</i>	3
<i>Stromal</i>	<i>Active normal</i>	5
<i>Stromal</i>	<i>Perturbed</i>	3
<i>Stromal</i>	<i>Active perturbed</i>	5
<i>Normal</i>	<i>Active normal</i>	15
<i>Normal</i>	<i>Perturbed</i>	3
<i>Normal</i>	<i>Active perturbed</i>	15
<i>Active normal</i>	<i>Perturbed</i>	15
<i>Active normal</i>	<i>Active perturbed</i>	15
<i>Perturbed</i>	<i>Active perturbed</i>	15

S4. *In vitro* experiments

Cell culture and transfection

HEK293T cells were purchased from Korean Cell Line Bank (Seoul National University, Seoul, Korea) and were maintained in Dulbecco's Modified Eagle's Medium (DMEM, PAA) supplemented with 10% heat-inactivated fetal bovine serum (FBS, Gibco) and 100 units/ml penicillin-streptomycin (Invitrogen). Cells were cultured at 37°C in a humidified 5% CO₂ atmosphere. Mycoplasma contamination of the cells was routinely evaluated using the e-Myco™ plus Mycoplasma PCR Detection Kit (Intron) according to the manufacturer's instructions.

Transfection of the CRD-BP expression vector (kindly provided by Dr. Jeff Ross, UW-Madison, WI) was performed using Lipofectamine 2000 (Invitrogen) in 96- and 6-well plates (SPL) according to the manufacturer's protocol. Briefly, Lipofectamine 2000 diluted in Opti-MEM® (Gibco) was applied to the plasmid diluted in Opti-MEM®, and the formulation was incubated for 25 min at room temperature. The culture medium was removed, and the mixture was applied to each well of the plates. After 6 h, the medium was changed to DMEM supplemented with 10% FBS. The vector pcDNA3.1 (Invitrogen) was used as a negative control.

esiRNA transfection was performed on HEK293T cells using the N-TER Nanoparticle siRNA Transfection System (Sigma) according to the manufacturer's instructions. Briefly, 2×10^4 or 4×10^5 HEK293T cells were seeded into each well of 96- or 6-well plates 18–24 h prior to transfection. The esiRNA nanoparticle formation solution (NFS) was prepared by adding *WWP2*, *BTRC*, *CRD-BP*, or control esiRNA (Sigma Aldrich; Cat# EHU059111, EHU069931, EHU020781, and SIC001, respectively) dilutions to N-TER Peptide dilutions, and the mixtures were incubated at room temperature

for 20 min. NFS transfection medium containing 50 nM target gene esiRNA was transferred to each well of the culture plates, and after 6 h, the medium was changed to DMEM supplemented with FBS.

RNA isolation and quantitative real-time polymerase chain reaction (qRT-PCR)

RNA extraction was performed 36 h after transfection and 1 h after TGF- β (Gibco; Cat# PHG9204) or WNT3a (R&D Systems; Cat# 5036-WN-010) incubation for the proper expression of Wwp2, β -TrCP1, or CRD-BP. Total RNA was isolated from transfected HEK293T cells using the RNA-spin™ Total RNA Extraction Kit (Intron), and the RNA was used to synthesize cDNA using the ImProm-II™ Reverse Transcription System (Promega). qRT-PCR was performed using iQ™ SYBR® Green Supermix (Bio-Rad), and the results were analyzed using a CFX Connect™ Real-Time PCR Detection System (Bio-Rad). All steps were performed according to the manufacturer's recommendations. The qRT-PCR thermal cycling was performed using an initial denaturation step at 95°C for 5 min followed by 40 cycles of denaturation at 95°C for 20 s, annealing at 60°C for 20 s, and elongation at 72°C for 20 s. For each qRT-PCR product, a single band of the expected size (approximately 100 bp) was observed using agarose gel electrophoresis (data not shown). The experiment was performed at least three times, and each qRT-PCR was performed in triplicate. The following primers were used for qRT-PCR:

mRNA	forward	reverse
<i>WWP2</i> (Wwp2)	5'-ACCGGCACTACACCAAGAAC-3'	5'-GCAGGTACCGGTGACAAACT-3'
<i>JUN</i> (c-Jun)	5'-CCCAAGATCCTGAAACAGA-3'	5'-GGTGAGGAGGTCCGAGTTCT-3'
<i>FGF2</i> (FGF2)	5'-GCGGCTGTACTGCAAAAACG-3'	5'-CTTGATGTGAGGGTCGCTCT-3'
<i>BTRC</i> (β -TrCP1)	5'-GGATTCCACGGTCAGAGTGT-3'	5'-TGCCATTATTGAAACGCAAG-3'
<i>CRD-BP</i> (CRD-BP)	5'-CTCCGATGGGAAGTACTGGA-3'	5'-CCGGTTGGAATAGGTGACAT-3'
<i>CCND1</i> (CyclinD1)	5'-CCCTCGGTGTCCTACTTCAA-3'	5'-CTCCTCGCACTTCTGTTCT-3'

Cell proliferation assay

A total of 1×10^4 HEK293T cells were plated in 96-well plates and cultured for 24 h. Subsequently, cells were transfected, and a medium containing TGF- β or WNT3a was used for proliferation assays. After 12 h (day 1), the number of cells was counted using a Cell Counting Kit-8 (Sigma) according to the manufacturer's instructions. The absorbance at 450 nm was measured using a microplate reader. The experiment was replicated at least three times, and each proliferation assay was performed in triplicate.

Cell migration assay

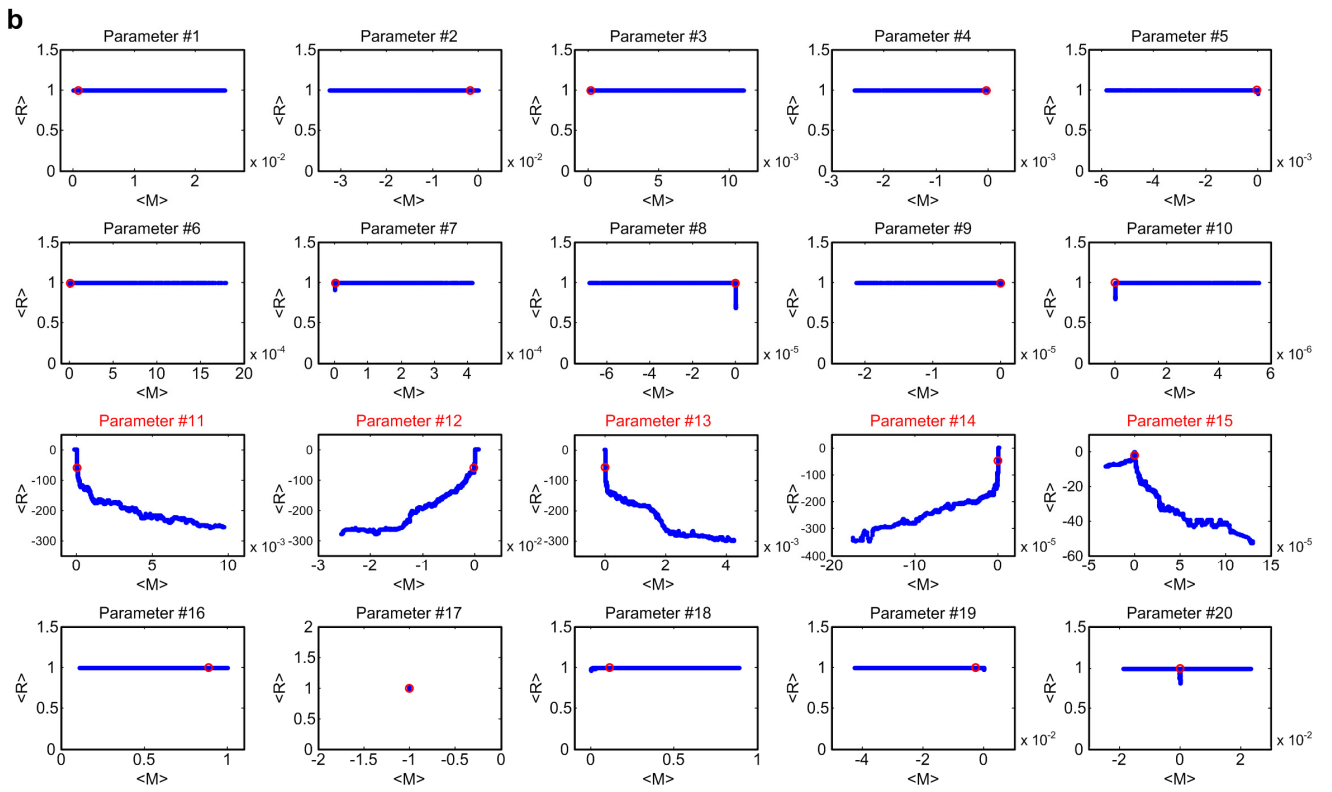
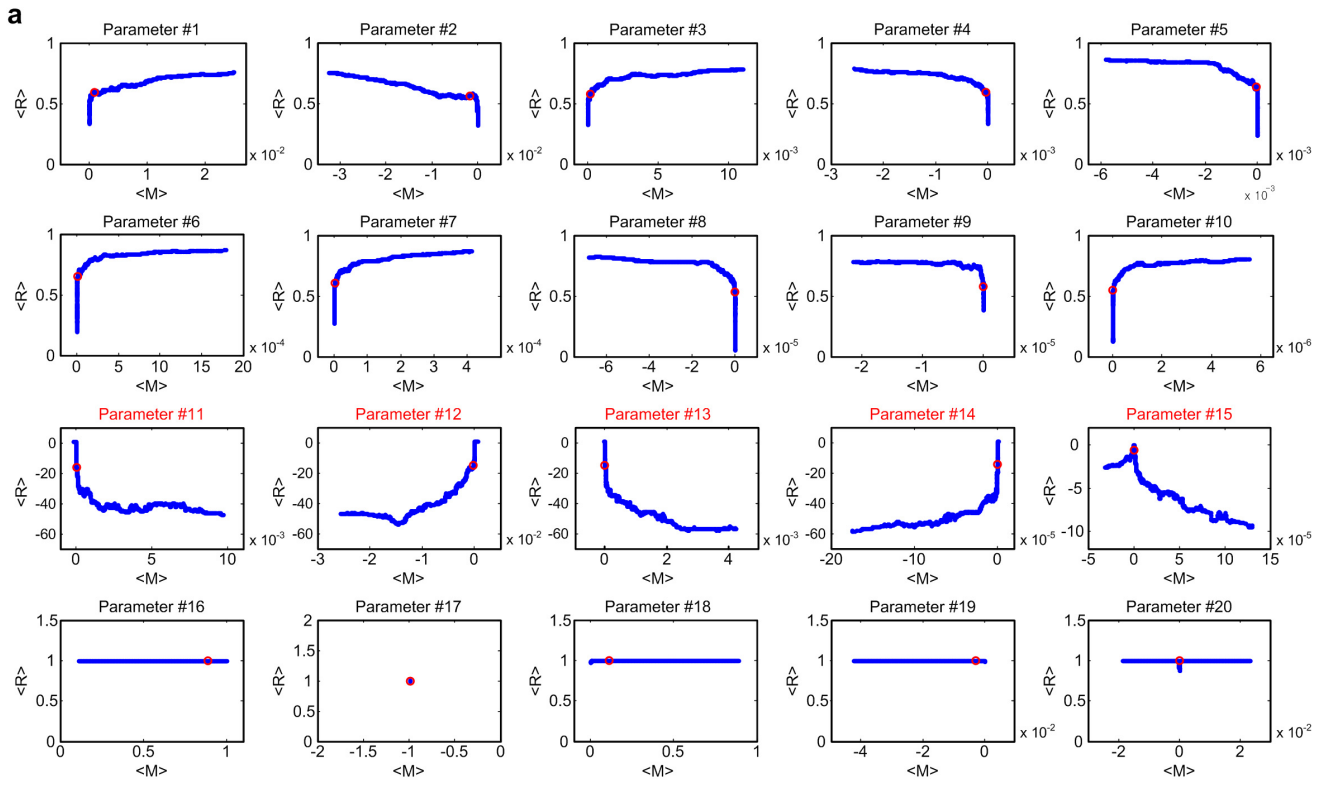
A migration assay was performed using the Cultrex 96-Well Cell Migration Assay (Trevigen Inc.) according to the manufacturer's instructions with minor modifications. Briefly, HEK293T cells at 80% confluence were seeded into the migration chamber after being starved in serum-free DMEM for 24 h. DMEM containing 10% FBS and TGF- β was added to the culture chamber to trigger cell migration. After 24 h of incubation at 37°C with 5% CO₂, the medium was removed, and both the migration and the culture chambers were washed with phosphate-buffered saline (PBS, Gibco). Subsequently, 500 μ l of cell dissociation solution/calcein-AM was added to the culture chamber of each well and incubated for 1 h. The migration chamber was subsequently discarded, and the dissociation solution/calcein-AM containing cells that were detached from the culture chamber was transferred to an assay chamber. Calcein fluorescence was measured using a Wallac 1420 Victor2 microplate reader (Perkin Elmer) at an excitation wavelength of 485 nm and an emission wavelength of 520 nm. A standard curve was generated to determine the number of migrated cells based on the fluorescence units. The experiment was replicated at least three times, and each migration assay was performed in triplicate.

II. Supplementary Notes

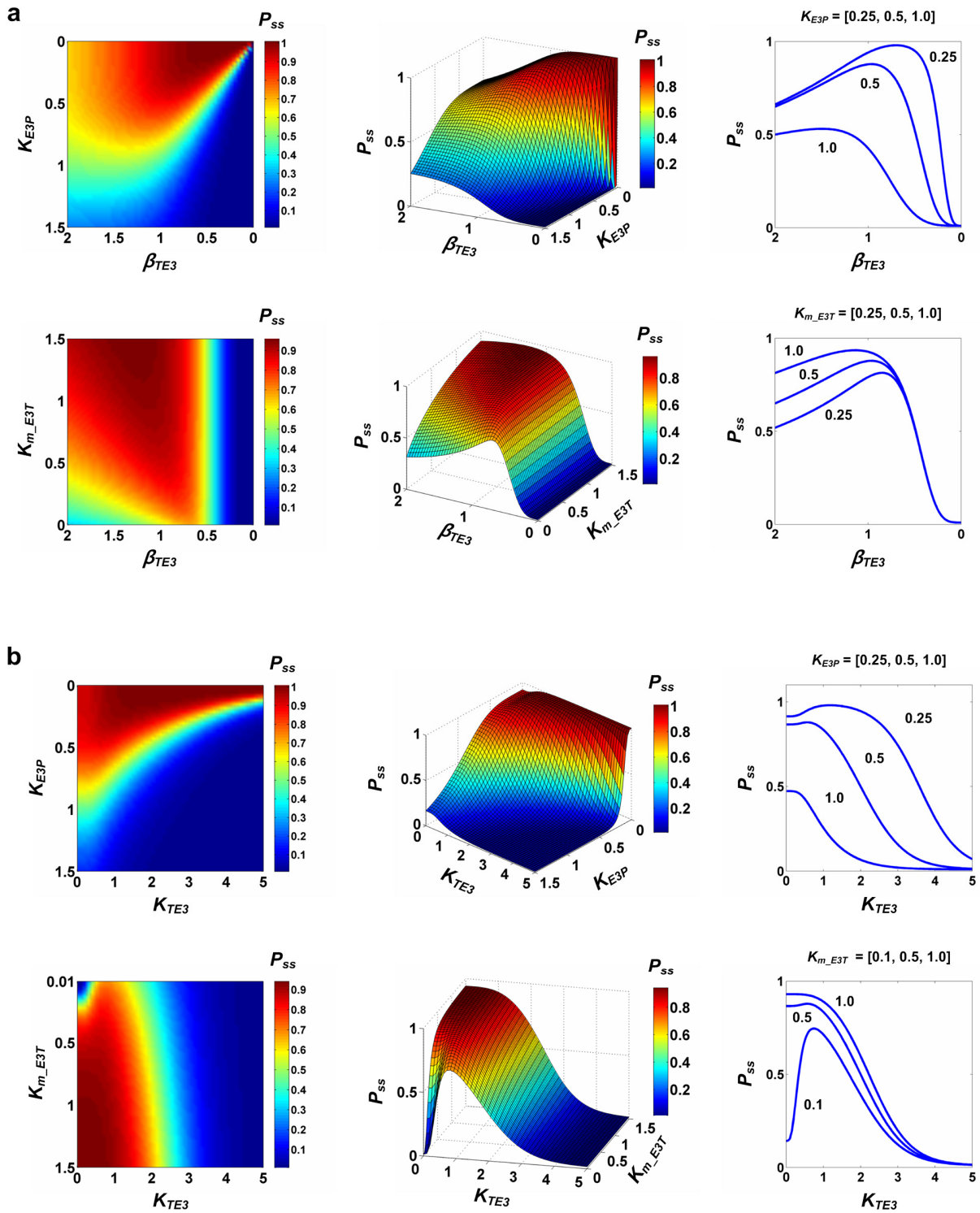
Supplementary Note 1. Limitation in preparing experimental systems

There is a limitation in preparing experimental systems that exactly correspond to the three mathematical models. We should manipulate the regulations such as $E3 \rightarrow P$ in a signaling pathway of ITUD to generate SNFL (or to generate ITUD from a signaling pathway of SNFL) and further need to find a component, I to realize DTUD. To realize SNFL from a signaling pathway of ITUD, for example, we might employ a protein engineering or use a specific inhibitor to disturb the interaction of E3 ubiquitin ligase with transcription complex for the expression of P . However, inhibiting $E3$ might also lose the ubiquitin ligase activity of $E3$ for UPS-dependent proteolysis of T since $E3$ can utilize the same domain for the proteolysis of T and transcriptional activation of P . In the case of β -catenin(T) and β -TrCP1($E3$), β -TrCP1 interacts with p300 for enhancing β -catenin transcriptional activity through WD40 domain³², which is also used to interact with the phosphorylated β -catenin (specifically, destruction motif called ‘degron’) for proteolytic ubiquitination⁹⁴. In the case of c-Myc(T) and Skp2($E3$), the ubiquitination of c-Myc is necessary for the transcriptional activation as well as the UPS-dependent proteolysis^{2,9}. Thus, preventing Skp2 from participating in transcription along with maintaining Skp2-mediated proteolysis of c-Myc requires an extremely difficult experimental strategy to realize the three experimental systems for ITUD and the alternative systems. Such difficulty might also apply to other signaling pathways.

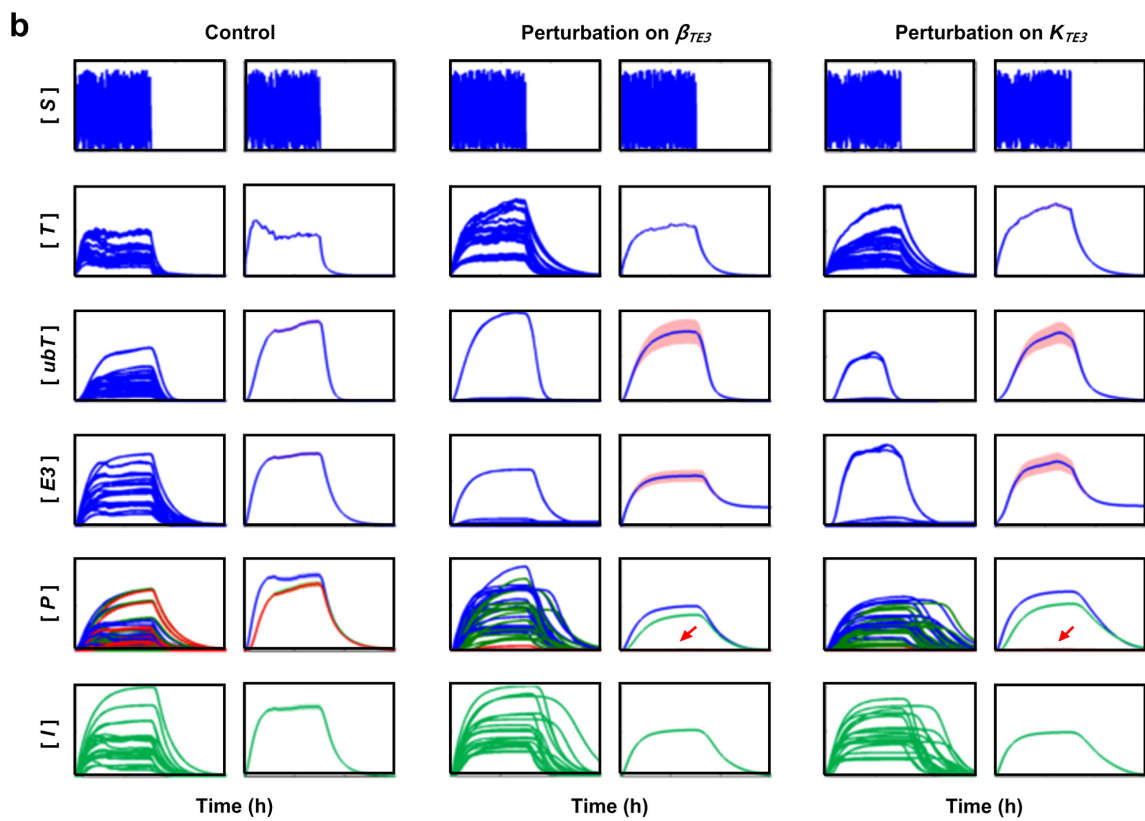
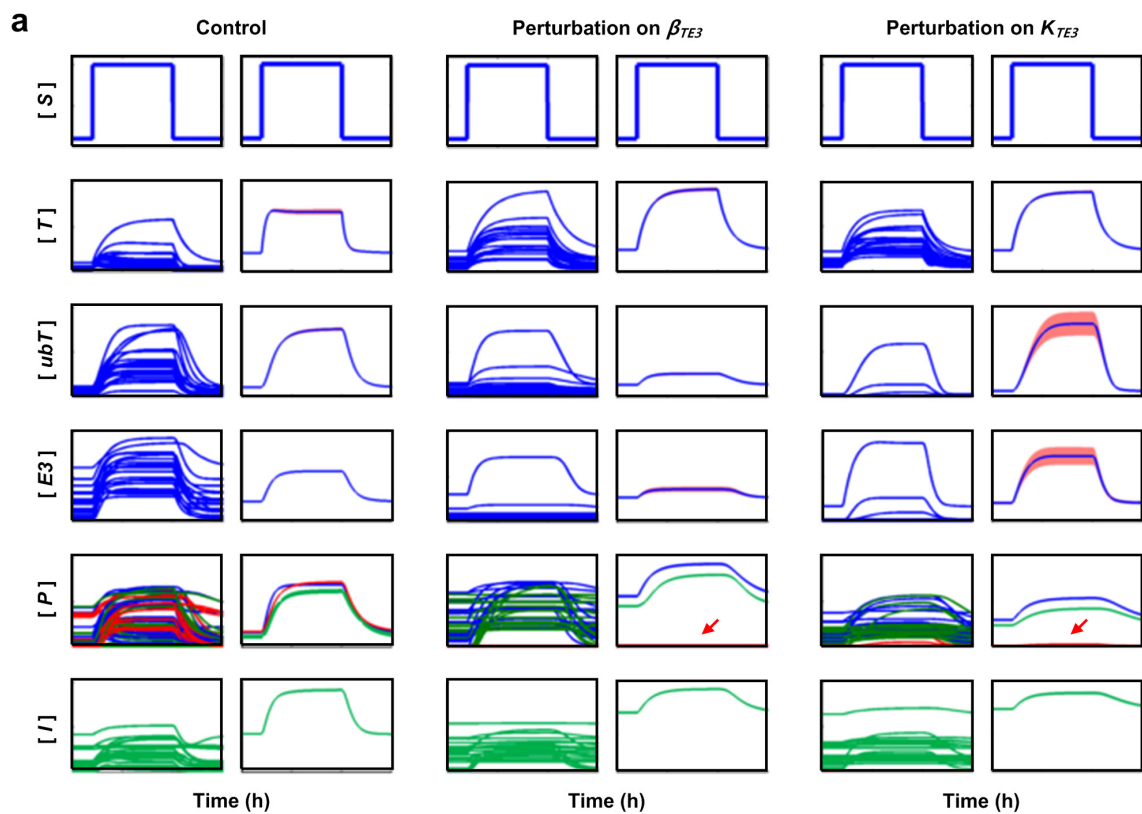
III. Supplementary Figures



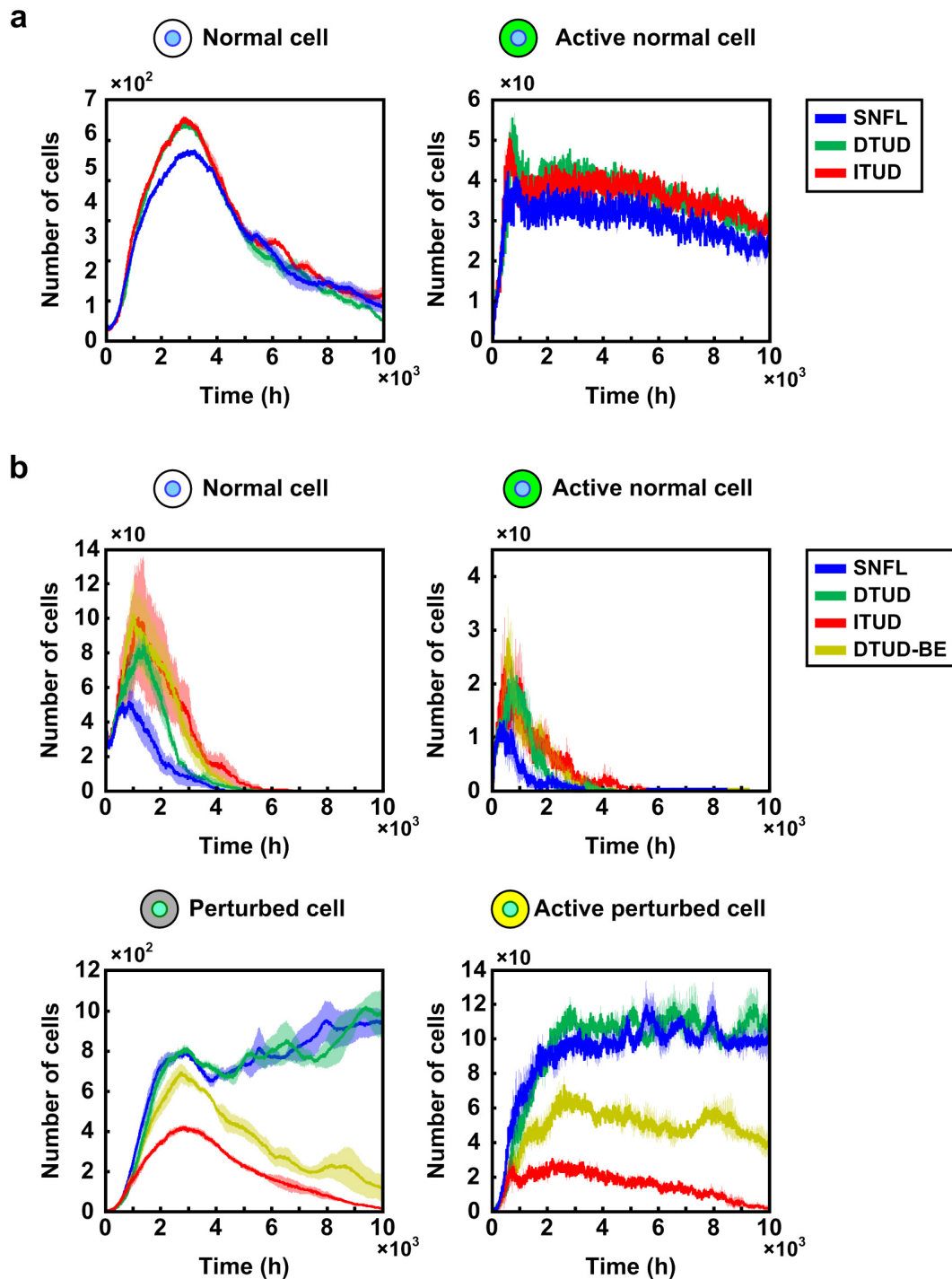
Supplementary Figure S1. Density plots for ratios of sensitivities over a wide range of parameter values. (a) The ratios of sensitivities between ITUD and SNFL, and (b) between ITUD and DTUD, obtained with a positive perturbation (+1%). (a-b) A larger absolute value of $\langle M \rangle$ (median of M_{ITUD}) means the output of ITUD system is more sensitive for a small change in a given parameter. If the median of the ratios ($\langle R \rangle$) is close to 1, it means the difference between ITUD and the compared system is very small. The density plots for the five parameters (ID:11-15, denoted as red) demonstrate that signs of the sensitivities between ITUD and the other two system are different and the absolute values of $\langle R \rangle$ are relatively large (i.e., >50). In contrast, those of the other parameters have the values of $\langle R \rangle$ within [0, 1]. In particular, the absolute values of $\langle R \rangle$ for the five parameters (ID:11-15) increase when ITUD system is very sensitive for the given parameters (i.e., $\langle M \rangle$ is large). It means the responses between ITUD and the compared system are very different with respect to the five parameters. The red circle denotes the point: (median of $\langle M \rangle$, median of $\langle R \rangle$). The results of negative perturbation (-1%) were similar to those of the positive perturbation.



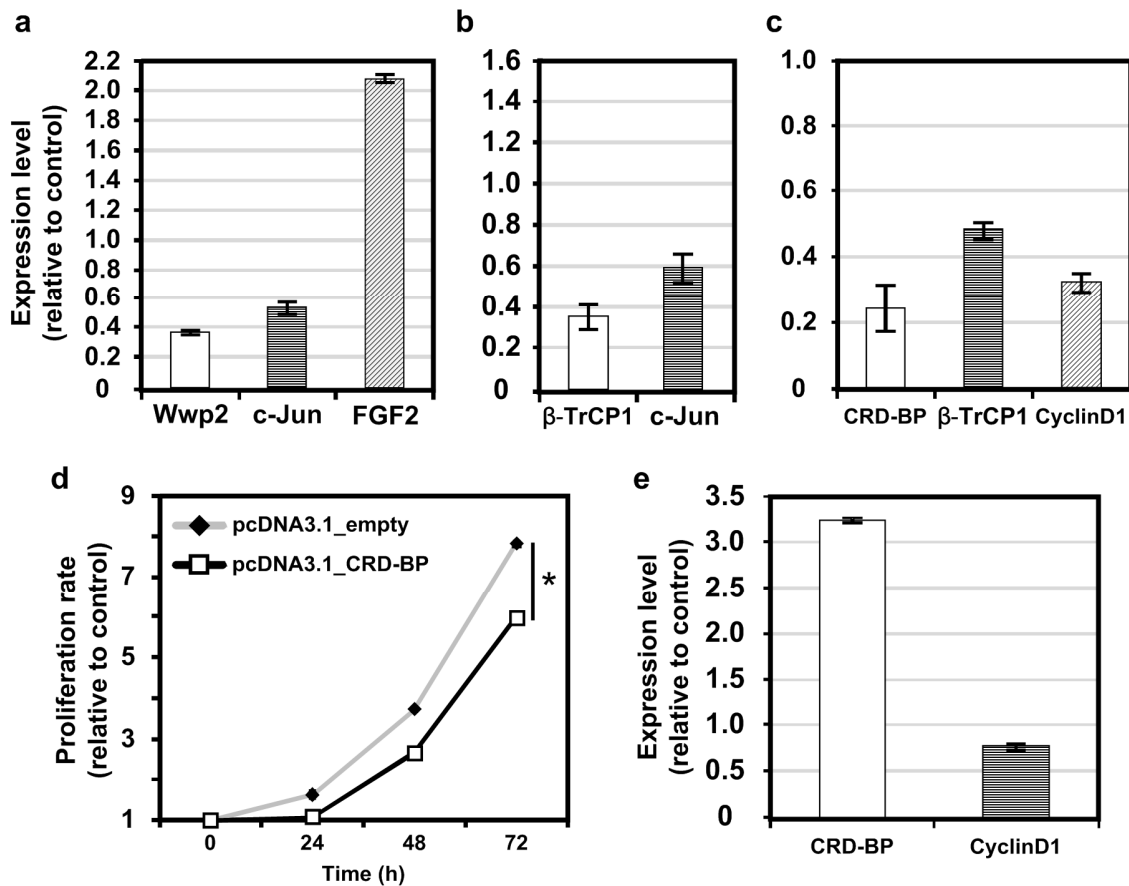
Supplementary Figure S2. Diverse shapes of the biphasic curves in ITUD system. We examined how the shapes of the biphasic response in ITUD system are affected by K_{m_E3T} and K_{E3P} under the perturbation of (a) β_{TE3} and (b) K_{TE3} . It demonstrates the tunability of the biphasic response in ITUD.



Supplementary Figure S3. Temporal dynamics over a wide range of parameter values with or without noise in signal. Temporal dynamics was obtained by increasing or decreasing the nominal parameter values randomly by 0~50%. In each perturbation condition, the left column shows individual curves from 20 simulations and the right column shows the mean temporal profile with standard errors (shade) of the 20 simulations. Signal S was given **(a)** without noise and **(b)** with noise. In the noise free condition, all the initial state values were numerically calculated with $S = 0.1$. In the noisy signal, all the initial state values were zeros. The perturbations are identical to those in Figure 5. The red arrows indicate the temporal profiles of P in ITUD.



Supplementary Figure S4. Temporal dynamics of each cell type in *in silico* analysis of cell proliferation. The temporal profiles from *in silico* analysis of cell proliferation dynamics (a) without (control) and (b) with the perturbation of the critical determinants in the subcellular pathway such as SNFL, DTUD, DTUD-BE, and ITUD. The shades around the curves are standard errors (n=3).



Supplementary Figure S5. Gene expression and cell proliferation assay. (a-c) We examined mRNA expression of target gene that promotes cell proliferation (c-Jun and CyclinD1) or mRNA expression of a gene that is related to cell migration (FGF2) under the downregulation of E3 ubiquitin ligases; knockdown of (a) Wwp2, (b) β -TrCP1, and (c) CRD-BP. (d) Proliferation rate of 293T cells under the overexpression of CRD-BP. (e) Expression of CyclinD1 under CRD-BP overexpression. (c-e) CRD-BP is an indirect regulator that stabilizes mRNA of β -TrCP1 in β -catenin pathway. Thus, knockdown and overexpression of CRD-BP are perturbations for β -TrCP1 expression, which correspond to the perturbations of β_{TE3} in the *in silico* analysis.

IV. Supplementary Tables

Supplementary Table S1. Mathematical models for SNFL, DTUD, and ITUD system. The numbers in brackets are parameter IDs. The dotted arrows represent the basal production or degradation rates. The red parts represent the critical determinants: β_{TE3} (ID: 13) and K_{TE3} (ID: 14). The ordinary differential equations for T , ubT , $E3$ of SNFL and DTUD are the same as those of ITUD.

Ordinary differential equations	
ITUD	$\frac{d[T]}{dt} = \beta_r - \alpha_T \cdot [T] + k_{ST} \frac{[S]}{K_{ST} + [S]} - k_{E3T} \cdot [E3] \cdot \frac{[T]}{K_{m_E3T} + [T]} + V_{m_ubT} \cdot \frac{[ubT]}{K_{m_ubT} + [ubT]}$ $\frac{d[ubT]}{dt} = -\alpha_T \cdot [ubT] + k_{E3T} \cdot [E3] \cdot \frac{[T]}{K_{m_E3T} + [T]} - V_{m_ubT} \cdot \frac{[ubT]}{K_{m_ubT} + [ubT]} - V_{m_pro} \cdot \frac{[ubT]}{K_{m_pro} + [ubT]}$ $\frac{d[E3]}{dt} = \beta_{E3} - \alpha_{E3} \cdot [E3] + \beta_{TE3} \cdot \frac{[T]^{n_{TE3}}}{K_{TE3}^{n_{TE3}} + [T]^{n_{TE3}}}$ $\frac{d[P]}{dt} = \beta_p - \alpha_p \cdot [P] + \beta_{TE3P} \cdot \left(\frac{[T]^{n_{TP}}}{K_{TP}^{n_{TP}} + [T]^{n_{TP}}} \right) \left(\frac{[E3]^{n_{E3P}}}{K_{E3P}^{n_{E3P}} + [E3]^{n_{E3P}}} \right)$
SNFL	$\frac{d[P]}{dt} = \beta_p - \alpha_p \cdot [P] + \beta_{TP} \cdot \left(\frac{[T]^{n_{TP}}}{K_{TP}^{n_{TP}} + [T]^{n_{TP}}} \right) \left(\frac{[T]^{n_{TP2}}}{K_{TP2}^{n_{TP2}} + [T]^{n_{TP2}}} \right)$

<p>DTUD</p>	$\frac{d[I]}{dt} = \beta_I - \alpha_I \cdot [I] + \beta_{TI} \cdot \frac{[T]^{n_T}}{K_{TI}^{n_T} + [T]^{n_T}}$ $\frac{d[P]}{dt} = \beta_P - \alpha_P \cdot [P] + \beta_{TIP} \cdot \left(\frac{[T]^{n_{TP}}}{K_{TP}^{n_{TP}} + [T]^{n_{TP}}} \right) \left(\frac{[I]^{n_{IP}}}{K_{IP}^{n_{IP}} + [I]^{n_{IP}}} \right)$
Components	
<p>S</p>	<p>S is an extracellular or intracellular signal which increases the amount of T.</p>
<p>T</p>	<p>T is a transcription factor which promotes the expression of target genes, E3 and P.</p>
<p>ubT</p>	<p>ubT is the poly-ubiquitinated state of T. The ubiquitination of T is promoted by E3, and ubT can undergo proteasomal degradation.</p>
<p>E3</p>	<p>E3 represents an E3 ubiquitin ligase. It not only promotes UPS-dependent proteolysis of T, but also participates in the transcription of P.</p>
<p>P</p>	<p>P is the final product, which is the output of the system.</p>
<p>I</p>	<p>I is an intermediate node that cooperates with T for the expression of P in DTUD.</p>

Supplementary Table S2. A set of the nominal values for kinetic parameters.

ID	Parameter	Reaction	SNFL	DTUD	ITUD	Unit
			Value			
Basal production/degradation						
1	β_T	Basal production of (<i>T</i>)	0.01			[level]·hour ⁻¹
2	α_T	Basal degradation of all states of (<i>T</i>)	1.0			hour ⁻¹
11	β_{E3}	Basal production of (<i>E3</i>)	0.01			[level]·hour ⁻¹
12	α_{E3}	Basal degradation of (<i>E3</i>)	1.0			hour ⁻¹
16	β_P	Basal production of (<i>P</i>)	0.01			[level]·hour ⁻¹
17	α_P	Basal degradation of (<i>P</i>)	1.0			hour ⁻¹
23	β_I	Basal production of (<i>I</i>)	–	0.01	–	[level]·hour ⁻¹
24	α_I	Basal degradation of (<i>I</i>)	–	1.0	–	hour ⁻¹
Rapid enzyme-substrate kinetics						
3	k_{ST}	Activation of (<i>T</i>)	5.0			[level]·hour ⁻¹
4	$K_{m\ ST}$	Activation of (<i>T</i>)	0.5			[level]
5	k_{E3T}	Ubiquitination of (<i>T</i>)	5.0			hour ⁻¹
6	$K_{m\ E3T}$	Ubiquitination of (<i>T</i>)	0.5			[level]
7	$V_{m\ ubT}$	Deubiquitination of (<i>ubT</i>)	1.0			[level]·hour ⁻¹
8	$K_{m\ ubT}$	Deubiquitination of (<i>ubT</i>)	0.5			[level]
9	$V_{m\ pro}$	Proteasomal degradation of (<i>ubT</i>)	1.0			[level]·hour ⁻¹
10	$K_{m\ pro}$	Proteasomal degradation of (<i>ubT</i>)	0.5			[level]
Transcriptional regulation						
13	β_{TE3}	Transactivation of (<i>E3</i>) by (<i>T</i>)	1.0			[level]·hour ⁻¹
14	K_{TE3}	Transactivation of (<i>E3</i>) by (<i>T</i>)	0.5			[level]
15	n_{TE3}	Transactivation of (<i>E3</i>) by (<i>T</i>)	4			dimensionless
25	β_{TI}	Transactivation of (<i>I</i>) by (<i>T</i>)	–	1.0	–	[level]·hour ⁻¹
26	K_{TI}	Transactivation of (<i>I</i>) by (<i>T</i>)	–	0.5	–	[level]
27	n_{TI}	Transactivation of (<i>I</i>) by (<i>T</i>)	–	4	–	dimensionless
18	$\beta_{TP}, \beta_{TIP}, \beta_{TE3P}$	Transactivation of (<i>P</i>) by (<i>T</i>), (<i>I</i>), or (<i>E3</i>)	1.0			[level]·hour ⁻¹
19	K_{TP}	Transactivation of (<i>P</i>) by (<i>T</i>)	0.5			[level]
20	n_{TP}	Transactivation of (<i>P</i>) by (<i>T</i>)	4			dimensionless
21	K_{TP2}, K_{IP}, K_{E3P}	Transactivation of (<i>P</i>) by (<i>T</i>), (<i>I</i>), or (<i>E3</i>)	0.5166	0.5	0.5	[level]
22	n_{TP2}, n_{IP}, n_{E3P}	Transactivation of (<i>P</i>) by (<i>T</i>), (<i>I</i>), or (<i>E3</i>)	4	4	4	dimensionless

V. Supplementary Movies

Movie S1. A representative movie of *in silico* cell proliferation dynamics without perturbation (control).

Movie S2. A representative movie of *in silico* cell proliferation dynamics under perturbation.

Movie S3. A representative movie of *in silico* cell migration dynamics under perturbation.

Movie S4. A representative movie for the diffusion field of signal S . The signal intensity value, 1.0, corresponds to the nominal value of the activating signal in a subcellular pathway such as SNFL, DTUD, and ITUD.

VI. Supplementary References

- 1 Chan, C. H. *et al.* Deciphering the transcriptional complex critical for RhoA gene expression and cancer metastasis. *Nat. Cell Biol.* **12**, 457-467; doi:10.1038/ncb2047 (2010).
- 2 von der Lehr, N. *et al.* The F-box protein Skp2 participates in c-Myc proteosomal degradation and acts as a cofactor for c-Myc-regulated transcription. *Mol. Cell* **11**, 1189-1200; doi:10.1016/S1097-2765(03)00193-X (2003).
- 3 Kodadek, T., Sikder, D. & Nalley, K. Keeping transcriptional activators under control. *Cell* **127**, 261-264; doi:10.1016/j.cell.2006.10.002 (2006).
- 4 Leung, A. *et al.* [Transcriptional control and the ubiquitin-proteasome system] *Ernst Schering Foundation Symposium Proceedings* (S. Jentsch & B. Haendler (eds)) [pp. 75-97] (Springer Berlin Heidelberg, 2008).
- 5 O'Malley, B. W., Qin, J. & Lanz, R. B. Cracking the coregulator codes. *Curr. Opin. Cell Biol.* **20**, 310-315; doi:10.1016/j.ceb.2008.04.005 (2008).
- 6 Geng, F., Wenzel, S. & Tansey, W. P. Ubiquitin and proteasomes in transcription. *Annu. Rev. Biochem.* **81**, 177-201; doi:10.1146/annurev-biochem-052110-120012 (2012).
- 7 Luscher, B. & Vervoorts, J. Regulation of gene transcription by the oncoprotein MYC. *Gene* **494**, 145-160; doi:10.1016/j.gene.2011.12.027 (2012).
- 8 Tansey, W. P. Transcriptional activation: risky business. *Genes Dev.* **15**, 1045-1050; doi:10.1101/gad.896501 (2001).
- 9 Kim, S. Y., Herbst, A., Tworkowski, K. A., Salghetti, S. E. & Tansey, W. P. Skp2 regulates Myc protein stability and activity. *Mol. Cell* **11**, 1177-1188; doi:10.1016/S1097-2765(03)00173-4 (2003).
- 10 Welcker, M. *et al.* The Fbw7 tumor suppressor regulates glycogen synthase kinase 3 phosphorylation-dependent c-Myc protein degradation. *Proc. Natl. Acad. Sci. U. S. A.* **101**, 9085-9090; doi:10.1073/pnas.0402770101 (2004).
- 11 Popov, N., Schulein, C., Jaenicke, L. A. & Eilers, M. Ubiquitylation of the amino terminus of Myc by SCF(beta-TrCP) antagonizes SCF(Fbw7)-mediated turnover. *Nat. Cell Biol.* **12**, 973-981; doi:10.1038/ncb2104 (2010).
- 12 Bretones, G. *et al.* SKP2 oncogene is a direct MYC target gene and MYC down-regulates p27(KIP1) through SKP2 in human leukemia cells. *J. Biol. Chem.* **286**, 9815-9825; doi:10.1074/jbc.M110.165977 (2011).
- 13 Qu, X. *et al.* A signal transduction pathway from TGF-beta1 to SKP2 via Akt1 and c-Myc and its correlation with progression in human melanoma. *J. Invest. Dermatol.* **134**, 159-167; doi:10.1038/jid.2013.281 (2014).
- 14 Lee, S. B. *et al.* Romo1 is a negative-feedback regulator of Myc. *J. Cell Sci.* **124**, 1911-1924; doi:10.1242/jcs.079996 (2011).
- 15 Buttica, C., Michielin, O., Wyniger, J., Telenti, A. & Rothenberger, S. Silencing of both beta-TrCP1 and HOS (beta-TrCP2) is required to suppress human immunodeficiency virus type 1 Vpu-mediated CD4 down-modulation. *J. Virol.* **81**, 1502-1505; doi:10.1128/JVI.01711-06 (2007).
- 16 Frescas, D. & Pagano, M. Deregulated proteolysis by the F-box proteins SKP2 and beta-TrCP: tipping the scales of cancer. *Nat. Rev. Cancer* **8**, 438-449; doi:10.1038/nrc2396 (2008).
- 17 Kafri, R., Springer, M. & Pilpel, Y. Genetic redundancy: new tricks for old genes. *Cell* **136**, 389-392; doi:10.1016/j.cell.2009.01.027 (2009).
- 18 Seo, E. *et al.* Multiple isoforms of beta-TrCP display differential activities in the regulation of Wnt signaling. *Cell. Signal.* **21**, 43-51; doi:10.1016/j.cellsig.2008.09.009 (2009).

- 19 Putters, J., Slotman, J. A., Gerlach, J. P. & Strous, G. J. Specificity, location and function of betaTrCP isoforms and their splice variants. *Cell. Signal.* **23**, 641-647; doi:10.1016/j.cellsig.2010.11.015 (2011).
- 20 Fuchs, S. Y., Spiegelman, V. S. & Kumar, K. G. The many faces of beta-TrCP E3 ubiquitin ligases: reflections in the magic mirror of cancer. *Oncogene* **23**, 2028-2036; doi:10.1038/sj.onc.1207389 (2004).
- 21 Kanarek, N. *et al.* Spermatogenesis rescue in a mouse deficient for the ubiquitin ligase SCF{beta}-TrCP by single substrate depletion. *Genes Dev.* **24**, 470-477; doi:10.1101/gad.551610 (2010).
- 22 MacDonald, B. T., Tamai, K. & He, X. Wnt/beta-catenin signaling: components, mechanisms, and diseases. *Dev. Cell* **17**, 9-26; doi:10.1016/j.devcel.2009.06.016 (2009).
- 23 Zhang, W. *et al.* PR55 alpha, a regulatory subunit of PP2A, specifically regulates PP2A-mediated beta-catenin dephosphorylation. *J. Biol. Chem.* **284**, 22649-22656; doi:10.1074/jbc.M109.013698 (2009).
- 24 Taya, S., Yamamoto, T., Kanai-Azuma, M., Wood, S. A. & Kaibuchi, K. The deubiquitinating enzyme Fam interacts with and stabilizes beta-catenin. *Genes Cells* **4**, 757-767; doi:10.1046/j.1365-2443.1999.00297.x (1999).
- 25 Sadot, E. *et al.* Regulation of S33/S37 phosphorylated beta-catenin in normal and transformed cells. *J. Cell Sci.* **115**, 2771-2780 (2002).
- 26 Spiegelman, V. S. *et al.* Wnt/beta-catenin signaling induces the expression and activity of betaTrCP ubiquitin ligase receptor. *Mol. Cell* **5**, 877-882; doi:10.1016/S1097-2765(00)80327-5 (2000).
- 27 Noubissi, F. K. *et al.* CRD-BP mediates stabilization of betaTrCP1 and c-myc mRNA in response to beta-catenin signalling. *Nature* **441**, 898-901; doi:10.1038/nature04839 (2006).
- 28 Elcheva, I., Goswami, S., Noubissi, F. K. & Spiegelman, V. S. CRD-BP protects the coding region of betaTrCP1 mRNA from miR-183-mediated degradation. *Mol. Cell* **35**, 240-246; doi:10.1016/j.molcel.2009.06.007 (2009).
- 29 Jho, E. H. *et al.* Wnt/beta-catenin/Tcf signaling induces the transcription of Axin2, a negative regulator of the signaling pathway. *Mol. Cell. Biol.* **22**, 1172-1183; doi:10.1016/S1097-2765(03)00090-X (2002).
- 30 Leung, J. Y. *et al.* Activation of AXIN2 expression by beta-catenin-T cell factor. A feedback repressor pathway regulating Wnt signaling. *J. Biol. Chem.* **277**, 21657-21665; doi:10.1074/jbc.M200139200 (2002).
- 31 Lustig, B. *et al.* Negative feedback loop of Wnt signaling through upregulation of conductin/Axin2 in colorectal and liver tumors. *Mol. Cell. Biol.* **22**, 1184-1193; doi:10.1128/Mcb.22.4.1184-1193.2002 (2002).
- 32 Kimbrel, E. A. & Kung, A. L. The F-box protein beta-TrCp1/Fbw1a interacts with p300 to enhance beta-catenin transcriptional activity. *J. Biol. Chem.* **284**, 13033-13044; doi:10.1074/jbc.M901248200 (2009).
- 33 Furumatsu, T., Tsuda, M., Taniguchi, N., Tajima, Y. & Asahara, H. Smad3 induces chondrogenesis through the activation of SOX9 via CREB-binding protein/p300 recruitment. *J. Biol. Chem.* **280**, 8343-8350; doi:10.1074/jbc.M413913200 (2005).
- 34 Furumatsu, T., Ozaki, T. & Asahara, H. Smad3 activates the Sox9-dependent transcription on chromatin. *Int. J. Biochem. Cell Biol.* **41**, 1198-1204; doi:10.1016/j.biocel.2008.10.032 (2009).
- 35 James, A. W., Xu, Y., Lee, J. K., Wang, R. & Longaker, M. T. Differential effects of TGF-beta1 and TGF-beta3 on chondrogenesis in posterofrontal cranial suture-derived mesenchymal cells in vitro. *Plast. Reconstr. Surg.* **123**, 31-43; doi:10.1097/PRS.0b013e3181904c19 (2009).

- 36 Mueller, M. B. *et al.* Hypertrophy in mesenchymal stem cell chondrogenesis: effect of TGF-beta isoforms and chondrogenic conditioning. *Cells Tissues Organs* **192**, 158-166; doi:10.1159/000313399 (2010).
- 37 Feng, X. H. & Derynck, R. Specificity and versatility in tgf-beta signaling through Smads. *Annu. Rev. Cell Dev. Biol.* **21**, 659-693; doi:10.1146/annurev.cellbio.21.022404.142018 (2005).
- 38 Lee, Y. J., Kong, M. H., Song, K. Y., Lee, K. H. & Heo, S. H. The Relation Between Sox9, TGF-beta1, and Proteoglycan in Human Intervertebral Disc Cells. *J. Korean Neurosurg. Soc.* **43**, 149-154; doi:10.3340/jkns.2008.43.3.149 (2008).
- 39 Kawakami, Y., Rodriguez-Leon, J. & Izpisua Belmonte, J. C. The role of TGFbetas and Sox9 during limb chondrogenesis. *Curr. Opin. Cell Biol.* **18**, 723-729; doi:10.1016/j.ceb.2006.10.007 (2006).
- 40 Zou, W. *et al.* The E3 ubiquitin ligase Wwp2 regulates craniofacial development through mono-ubiquitylation of Goosecoid. *Nat. Cell Biol.* **13**, 59-65; doi:10.1038/ncb2134 (2011).
- 41 Nakamura, Y. *et al.* Wwp2 is essential for palatogenesis mediated by the interaction between Sox9 and mediator subunit 25. *Nat Commun* **2**, 251; doi:10.1038/ncomms1242 (2011).
- 42 Soond, S. M. & Chantry, A. Selective targeting of activating and inhibitory Smads by distinct WWP2 ubiquitin ligase isoforms differentially modulates TGFbeta signalling and EMT. *Oncogene* **30**, 2451-2462; doi:10.1038/onc.2010.617 (2011).
- 43 Chantry, A. WWP2 ubiquitin ligase and its isoforms New biological insight and promising disease targets. *Cell Cycle* **10**, 2437-2439; doi:10.4161/cc.10.15.16874 (2011).
- 44 Labbe, E., Silvestri, C., Hoodless, P. A., Wrana, J. L. & Attisano, L. Smad2 and Smad3 positively and negatively regulate TGF beta-dependent transcription through the forkhead DNA-Binding protein FAST2. *Mol. Cell* **2**, 109-120; doi:10.1016/S1097-2765(00)80119-7 (1998).
- 45 Zhang, M. *et al.* Smad3 prevents beta-catenin degradation and facilitates beta-catenin nuclear translocation in chondrocytes. *J. Biol. Chem.* **285**, 8703-8710; doi:10.1074/jbc.M109.093526 (2010).
- 46 Wan, M. *et al.* SCF(beta-TrCP1) controls Smad4 protein stability in pancreatic cancer cells. *Am. J. Pathol.* **166**, 1379-1392 (2005).
- 47 Fukuchi, M. *et al.* Ligand-dependent degradation of Smad3 by a ubiquitin ligase complex of ROC1 and associated proteins. *Mol. Biol. Cell* **12**, 1431-1443 (2001).
- 48 Wan, M. *et al.* Smad4 protein stability is regulated by ubiquitin ligase SCF beta-TrCP1. *J. Biol. Chem.* **279**, 14484-14487; doi:10.1074/jbc.C400005200 (2004).
- 49 Proctor, C. J., Tsirigotis, M. & Gray, D. A. An in silico model of the ubiquitin-proteasome system that incorporates normal homeostasis and age-related decline. *BMC Syst. Biol.* **1**, 17; doi:10.1186/1752-0509-1-17 (2007).
- 50 Pierce, N. W., Kleiger, G., Shan, S. O. & Deshaies, R. J. Detection of sequential polyubiquitylation on a millisecond timescale. *Nature* **462**, 615-619; doi:10.1038/nature08595 (2009).
- 51 Mengel, B. *et al.* Modeling oscillatory control in NF-kappaB, p53 and Wnt signaling. *Curr. Opin. Genet. Dev.* **20**, 656-664; doi:10.1016/j.gde.2010.08.008 (2010).
- 52 Xu, L. & Qu, Z. Roles of protein ubiquitination and degradation kinetics in biological oscillations. *PLoS One* **7**, e34616; doi:10.1371/journal.pone.0034616 (2012).
- 53 Berg, J. M., Tymoczko, J. L. & Stryer, L. [Ch. 8. Enzymes: Basic Concepts and Kinetics] *Biochemistry* 6th ed. [pp. 216-225] (W.H. Freeman, 2012).
- 54 Michaelis, L., Menten, M. L., Johnson, K. A. & Goody, R. S. The original Michaelis constant: translation of the 1913 Michaelis-Menten paper. *Biochemistry* **50**, 8264-8269; doi:10.1021/bi201284u (2011).

- 55 Briggs, G. E. & Haldane, J. B. A Note on the Kinetics of Enzyme Action. *Biochem. J.* **19**, 338-339 (1925).
- 56 Chen, W. W., Niepel, M. & Sorger, P. K. Classic and contemporary approaches to modeling biochemical reactions. *Genes Dev.* **24**, 1861-1875; doi:10.1101/gad.1945410 (2010).
- 57 Alon, U. [Ch. 2. Transcription Networks: Basic Concepts] *An Introduction to Systems Biology: Design Principles of Biological Circuits* [p. 11] (Chapman & Hall/CRC, 2007).
- 58 Rose, Z. B. & Dube, S. Rates of phosphorylation and dephosphorylation of phosphoglycerate mutase and bisphosphoglycerate synthase. *J. Biol. Chem.* **251**, 4817-4822 (1976).
- 59 Strayhorn, W. D. & Wadzinski, B. E. A novel in vitro assay for deubiquitination of I kappa B alpha. *Arch. Biochem. Biophys.* **400**, 76-84; doi:10.1006/abbi.2002.2760 (2002).
- 60 Wang, X., Errede, B. & Elston, T. C. Mathematical analysis and quantification of fluorescent proteins as transcriptional reporters. *Biophys. J.* **94**, 2017-2026; doi:10.1529/biophysj.107.122200 (2008).
- 61 Korinek, V. *et al.* Constitutive transcriptional activation by a beta-catenin-Tcf complex in APC(-/-) colon carcinoma. *Science* **275**, 1784-1787; doi:10.1126/science.275.5307.1784 (1997).
- 62 Markowitz, S. D. & Bertagnolli, M. M. Molecular origins of cancer: Molecular basis of colorectal cancer. *N. Engl. J. Med.* **361**, 2449-2460; doi:10.1056/NEJMra0804588 (2009).
- 63 Skaar, J. R., D'Angiolella, V., Pagan, J. K. & Pagano, M. SnapShot: F Box Proteins II. *Cell* **137**, 1358, 1358 e1351; doi:10.1016/j.cell.2009.05.040 (2009).
- 64 Skaar, J. R., Pagan, J. K. & Pagano, M. SnapShot: F box proteins I. *Cell* **137**, 1160-1160 e1161; doi:10.1016/j.cell.2009.05.039 (2009).
- 65 Alberts, B. *et al.* [Ch. 6. How Cells Read the Genome: From DNA to Protein] *Molecular Biology of the Cell* 5th ed. [pp. 391-396] (Garland Science, 2008).
- 66 Reid, G. *et al.* Cyclic, proteasome-mediated turnover of unliganded and liganded ERalpha on responsive promoters is an integral feature of estrogen signaling. *Mol. Cell* **11**, 695-707; doi:10.1016/S1097-2765(03)00090-X (2003).
- 67 Lipford, J. R. & Deshaies, R. J. Diverse roles for ubiquitin-dependent proteolysis in transcriptional activation. *Nat. Cell Biol.* **5**, 845-850; doi:10.1038/ncb1003-845 (2003).
- 68 Mangan, S. & Alon, U. Structure and function of the feed-forward loop network motif. *Proc. Natl. Acad. Sci. U. S. A.* **100**, 11980-11985; doi:10.1073/pnas.2133841100 (2003).
- 69 Novak, B. & Tyson, J. J. Design principles of biochemical oscillators. *Nat. Rev. Mol. Cell Biol.* **9**, 981-991; doi:10.1038/nrm2530 (2008).
- 70 Verma, S. *et al.* The ubiquitin-conjugating enzyme UBC7 acts as a coactivator for steroid hormone receptors. *Mol. Cell. Biol.* **24**, 8716-8726; doi:10.1128/MCB.24.19.8716-8726.2004 (2004).
- 71 Lin, H. K. *et al.* Phosphorylation-dependent regulation of cytosolic localization and oncogenic function of Skp2 by Akt/PKB. *Nat. Cell Biol.* **11**, 420-432; doi:10.1038/ncb1849 (2009).
- 72 Inuzuka, H. *et al.* Acetylation-dependent regulation of Skp2 function. *Cell* **150**, 179-193; doi:10.1016/j.cell.2012.05.038 (2012).
- 73 Alon, U. [Ch. 4. The Feed-Forward Loop Network Motif] *An Introduction to Systems Biology: Design Principles of Biological Circuits* [pp. 41-73] (Chapman & Hall/CRC, 2007).
- 74 Kim, T. H., Jung, S. H. & Cho, K. H. Interlinked mutual inhibitory positive feedbacks induce robust cellular memory effects. *FEBS Lett.* **581**, 4899-4904; doi:10.1016/j.febslet.2007.09.020 (2007).
- 75 Kim, J. R., Yoon, Y. & Cho, K. H. Coupled feedback loops form dynamic motifs of cellular networks. *Biophys. J.* **94**, 359-365; doi:10.1529/biophysj.107.105106 (2008).

- 76 Kim, J. R., Shin, D., Jung, S. H., Heslop-Harrison, P. & Cho, K. H. A design principle underlying the synchronization of oscillations in cellular systems. *J. Cell Sci.* **123**, 537-543; doi:10.1242/jcs.060061 (2010).
- 77 Ratushny, A. V., Saleem, R. A., Sitko, K., Ramsey, S. A. & Aitchison, J. D. Asymmetric positive feedback loops reliably control biological responses. *Mol. Syst. Biol.* **8**, 577; doi:10.1038/msb.2012.10 (2012).
- 78 Shin, S. Y. *et al.* Positive- and negative-feedback regulations coordinate the dynamic behavior of the Ras-Raf-MEK-ERK signal transduction pathway. *J. Cell Sci.* **122**, 425-435; doi:10.1242/jcs.036319 (2009).
- 79 Shin, S. Y., Yang, H. W., Kim, J. R., Heo, W. D. & Cho, K. H. A hidden incoherent switch regulates RCAN1 in the calcineurin-NFAT signaling network. *J. Cell Sci.* **124**, 82-90; doi:10.1242/jcs.076034 (2011).
- 80 Won, J. K. *et al.* The crossregulation between ERK and PI3K signaling pathways determines the tumoricidal efficacy of MEK inhibitor. *J. Mol. Cell. Biol.* **4**, 153-163; doi:10.1093/jmcb/mjs021 (2012).
- 81 Sauro, H. M. [Ch. 9. Kinetics of Gene Regulation] *Enzyme Kinetics for Systems Biology* 1st ed. [pp. 203-248] (Ambrosius Publishing, 2011).
- 82 Weiss, J. N. The Hill equation revisited: uses and misuses. *FASEB J.* **11**, 835-841 (1997).
- 83 Alon, U. [Ch. 2. Transcription Networks: Basic Concepts] *An Introduction to Systems Biology: Design Principles of Biological Circuits* [pp. 13-15] (Chapman & Hall/CRC, 2007).
- 84 Savageau, M. A. [Ch. 10. Genetic Regulation: Repressible Systems] *Biochemical Systems Analysis: A Study of Function and Design in Molecular Biology* [pp. 306-334] (Addison-Wesley Pub. Co., Advanced Book Program, 1976).
- 85 Alves, R. & Savageau, M. A. Comparing systemic properties of ensembles of biological networks by graphical and statistical methods. *Bioinformatics* **16**, 527-533; doi:10.1093/bioinformatics/16.6.527 (2000).
- 86 Alon, U. [Ch. 3. Autoregulation: A Network Motif] *An Introduction to Systems Biology: Design Principles of Biological Circuits* [pp. 33-34] (Chapman & Hall/CRC, 2007).
- 87 Cickovski, T. *et al.* From Genes to Organisms Via the Cell A Problem-Solving Environment for Multicellular Development. *Comput Sci Eng* **9**, 50-60; doi:10.1109/MCSE.2007.74 (2007).
- 88 Graner, F. & Glazier, J. A. Simulation of biological cell sorting using a two-dimensional extended Potts model. *Phys. Rev. Lett.* **69**, 2013-2016; doi:10.1103/PhysRevLett.69.2013 (1992).
- 89 Andasari, V., Roper, R. T., Swat, M. H. & Chaplain, M. A. Integrating intracellular dynamics using CompuCell3D and Bionetsolver: applications to multiscale modelling of cancer cell growth and invasion. *PLoS One* **7**, e33726; doi:10.1371/journal.pone.0033726 (2012).
- 90 Jorgensen, P. & Tyers, M. How cells coordinate growth and division. *Curr. Biol.* **14**, R1014-1027; doi:10.1016/j.cub.2004.11.027 (2004).
- 91 Tzur, A., Kafri, R., LeBleu, V. S., Lahav, G. & Kirschner, M. W. Cell growth and size homeostasis in proliferating animal cells. *Science* **325**, 167-171; doi:10.1126/science.1174294 (2009).
- 92 Rozario, T. & DeSimone, D. W. The extracellular matrix in development and morphogenesis: a dynamic view. *Dev. Biol.* **341**, 126-140; doi:10.1016/j.ydbio.2009.10.026 (2010).
- 93 Roussos, E. T., Condeelis, J. S. & Patsialou, A. Chemotaxis in cancer. *Nat. Rev. Cancer* **11**, 573-587; doi:10.1038/nrc3078 (2011).
- 94 Wu, G. *et al.* Structure of a beta-TrCP1-Skp1-beta-catenin complex: destruction motif binding and lysine specificity of the SCF(beta-TrCP1) ubiquitin ligase. *Mol. Cell* **11**, 1445-1456; doi:10.1016/S1097-2765(03)00234-X (2003).